PERGAMON

Journal of Structural Geology 24 (2002) 155–172

JOURNAL OF STRUCTURAL GEOLOGY

www.elsevier.com/locate/jstrugeo

The state of stress in the limb of the Split Mountain anticline, Utah: constraints placed by transected joints

Laura J. Silliphant[a,1], Terry Engelder[a,*], Michael R. Gross[b]

[a]Department of Geosciences, The Pennsylvania State University, University Park, PA 16802, USA
[b]Department of Geology, Florida International University, Miami, FL 33199, USA

Received 9 August 2000; revised 22 February 2001; accepted 20 March 2001

Abstract

Transected joints (i.e. systematic joints that strike at an angle to the present fold axis trend) occur on the flanks of Split Mountain, a Laramide anticline near the eastern end of the Uinta Mountains, Utah. The common orientation on both flanks for these WNW-striking joints is inconsistent with joints driven by a syn-folding stretch normal to the direction of highest curvature. A smaller dispersion of the poles to these transected joints occurs when they are rotated with bedding to their 'pre-fold' orientation. This dispersion of poles is inconsistent with a post-fold genesis in a regional stress field but permits the possibility that these WNW joints propagated as a systematic set prior to Laramide folding. A pre-fold interpretation is substantiated by a regional WNW-striking joint set within Cretaceous and older rocks in the surrounding Piceance, Uinta, and southeastern Sand Wash basins. During tilting accompanying the upfolding of Split Mountain, most joints of this WNW-striking regional set remain locked without slipping under a shear stress. Fracture toughness and frictional strength are two rock properties that serve to lock a joint until a critical resolved shear stress is achieved. A gravity load caused down-dip slip on some joints that were tilted to a dip of about 62°. This suggests that a local principal stress remained roughly vertical during bedding rotation. Assuming fracture strength and friction prevented slip on most joints during tilting, the ratio of least horizontal, S_h, to vertical stress, S_v, at the critical tilt angle was approximately 0.55.

Keywords: Joints; Fractures; Forced fold; Transected joints; Faulted joints

1. Introduction

New techniques for the 3-D representation, reconstruction, and forward modeling of fault-related folds must be dynamically admissible. This is to say that 3-D models must remain consistent with the state of stress during the folding of natural rocks. A question then arises as to what constraints can be placed on stress in the limbs of a fold during the folding process. Our objective is to describe one technique for constraining the state of stress within the limb of the Split Mountain anticline, Utah, a fold attributed to Laramide deformation in the sense of both timing and style (Gries, 1983; Hansen, 1986).

We chose a Laramide-age structure for our study of stress in fold limbs, in part, to question the common perception that joint density always correlates with fold curvature in Laramide-style folds (Lisle, 1994; Engelder et al., 1997). Presumably, a correlation between joint density and fold curvature arises because an effective tensile stress is generated by tangential longitudinal strain during folding (e.g. Ramsay, 1967; Price and Cosgrove, 1990; Bobillo-Ares et al., 2000). This tension leads to the development of hinge-parallel fractures in the outer arc of the fold where the stretching direction is normal to the fold axis in folds with a 2-D evolution in fold shape (Ramsay and Huber, 1987; Lemiszki et al., 1994). In folds with a 3-D evolution in fold shape, joints may be induced by local fold-related strains that are neither parallel nor perpendicular to the fold axis (Fischer and Wilkerson, 2000). Early studies of the association between jointing and Laramide folding include those at Sheep Mountain and Goose Egg Dome, Wyoming (Harris et al., 1960), Williston Basin, North Dakota (Murray, 1968), Elk Basin, Montana (McCaleb and Wayhan, 1969), and Little Sand Draw, Wyoming (Garfield et al., 1992). Later studies have suggested that primary joint patterns at, for example, Sheep Mountain may reflect a former structural position (Maschmeyer and Cooke, 2000). Recent analyses calculating 3-D or Gaussian curvature of beds (e.g. Lisle, 1994) suggest that fold-related fracture density increases

* Corresponding author. Tel.: +1-814-865-3620; fax: +1-814-863-7823.
E-mail address: engelder@geosc.psu.edu (T. Engelder).
[1] Now at Anadarko Petroleum Corporation, Houston, TX 77251-1330, USA.

0191-8141/02/$ - see front matter
PII: S0191-8141(01)00055-4

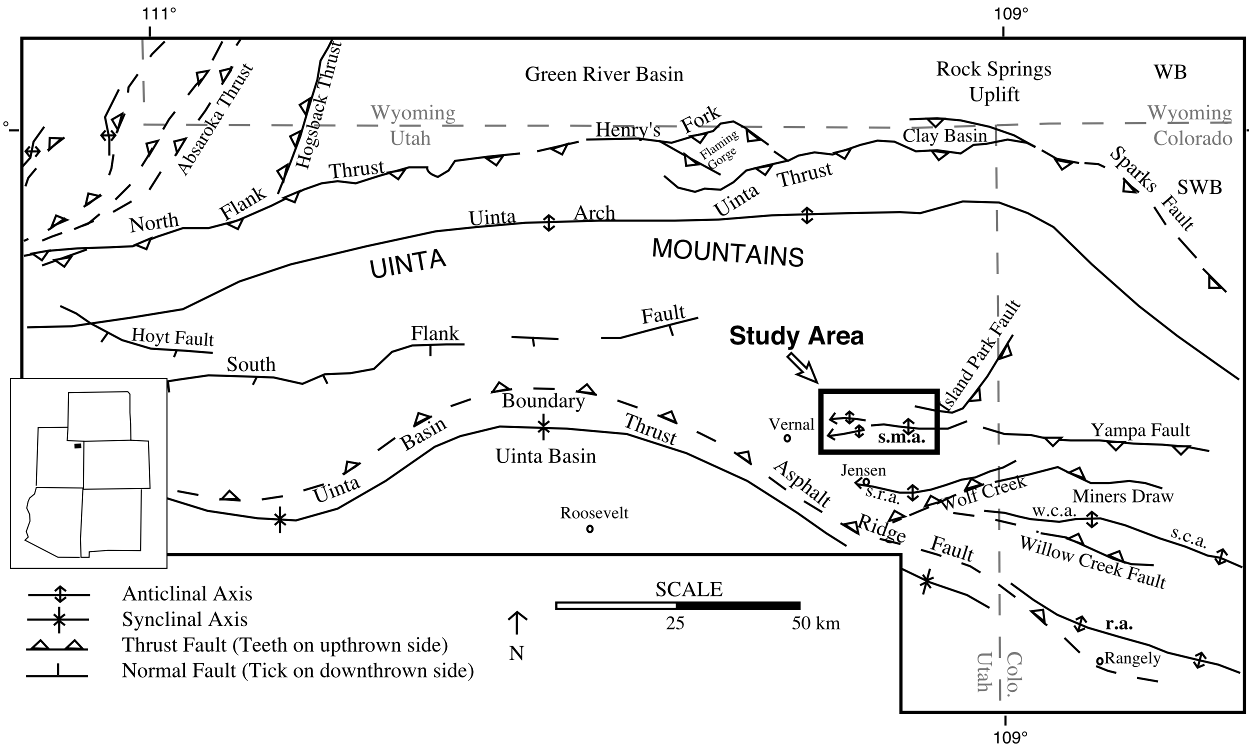

Fig. 1. Generalized tectonic map of the Uinta Mountains. WB = Washakie basin; SWB = Sand Wash basin; s.m.a. = Split Moutain anticline; s.r.a. = Section Ridge anticline; w.c.a. = Willow Creek anticline; s.c.a. = Skull Creek anticline; r.a. = Rangely anticline. Tectonic map was modified from Untermann and Untermann (1949), Ritzma (1969), Campbell (1975) and Bradley (1995).

with folding strain at Point Arguello, California (Narr, 1991) and Oil Mountain, Wyoming (Hennings et al., 2000).

Many Laramide-age structures are molded by the shape and trend of some forcing member such as a basement block and are consequently called forced folds (George Sowers, personal communication, 1971). This fold style, also referred to as a drape fold, is a specific example of a more general fold class (Stearns, 1978). Kinematically, forced folds have properties of leading-edge folds (e.g. Fisher and Anastasio, 1994), and are distinct from fault-propagation folds, which exhibit self-similar growth (Suppe, 1985; van der Pluijm and Marshak, 1997). The forcing member in a leading-edge fold is often not basement but rather a bend in a fault surface or a fault-related fold deeper within the sedimentary cover (Jamison, 1987; Cosgrove and Ameen, 2000). Draping over a forcing member can involve stretching of beds by deformation mechanisms varying from jointing (e.g. Engelder et al., 1997) to faulting (Withjack et al., 1990) to extreme cataclasis (e.g. Jamison and Stearns, 1982). Despite abundant data supporting the density–curvature hypothesis, not all well-developed joint sets about forced folds are generated by a fold-related mechanism. The purpose of this paper is to demonstrate that forced folding can take place without causing synfold jointing and without driving slip on most pre-existing transected joints. This behavior places a constraint on the state of stress within fold limbs during folding.

Transected joints are a set of systematic joints that trend at some angle to the present fold axis and form either before folding or during an early stage of folding. Transected joints on opposite flanks of a fold appear as a single, systematic set only when bedding is restored to its original attitude. Later tightening of the fold causes the joint set to fan about the flanks of the fold and thereby increases the scatter of poles to systematic joints, in contrast to the tight clustering of poles to a systematic joint set that might be found in uniformly dipping rocks. The term, transected joints, comes from the literature on cleavage where *transected cleavage* occurs at a distinct angle with the fold hinge (e.g. Ramsay and Huber, 1987, p. 334). A transected cleavage is not necessarily a late generation of cleavage superimposed on folding but rather it may be a cleavage from any stage of the folding process (Powell, 1974; Treagus and Treagus, 1981; Ghosh, 1993).

2. The geology of Split Mountain anticline

This paper presents new field data on brittle fracture about the Split Mountain anticline, Dinosaur National Monument, Utah, a west-plunging forced fold that formed during the Eocene uplift of the Eastern Uinta Mountains (Figs. 1–3). Interest in fractures at Split Mountain anticline stems from its similarity to Rangely anticline, Colorado, a prolific reservoir in a Laramide fold 60 km to the southeast (Fig. 1). The Rangely structure is a two billion barrel oil

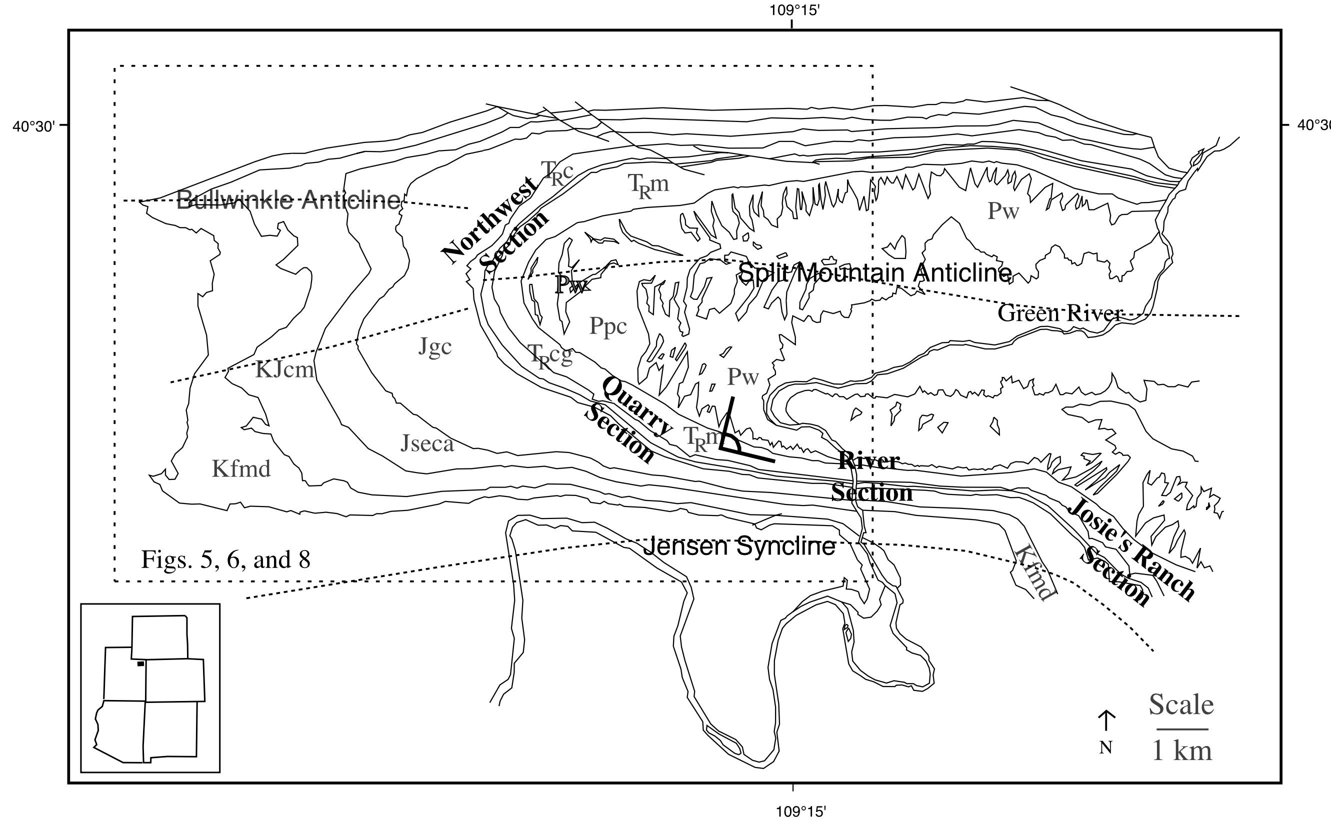

Fig. 2. Geologic map of Split Mountain anticline showing the structural sections referred to in this paper. Eye icon indicates the position of the view looking to the NE in Fig. 3. Lithologic map symbols are as follows: Kfmd = Frontier Sandstone, Mowry Shale, Dakota Formation; KJcm = Cedar Mountain Formation, Morrison Formation; Jseca = Stump Formation, Entrada Sandstone, Carmel Formation; Jgc = Glen Canyon Group; T_Rc = Chinle Formation; T_Rcg = Gartra Member of Chinle; T_Rm = Moenkopi Formation; Ppc = Park City Formation; Pw = Weber Sandstone.

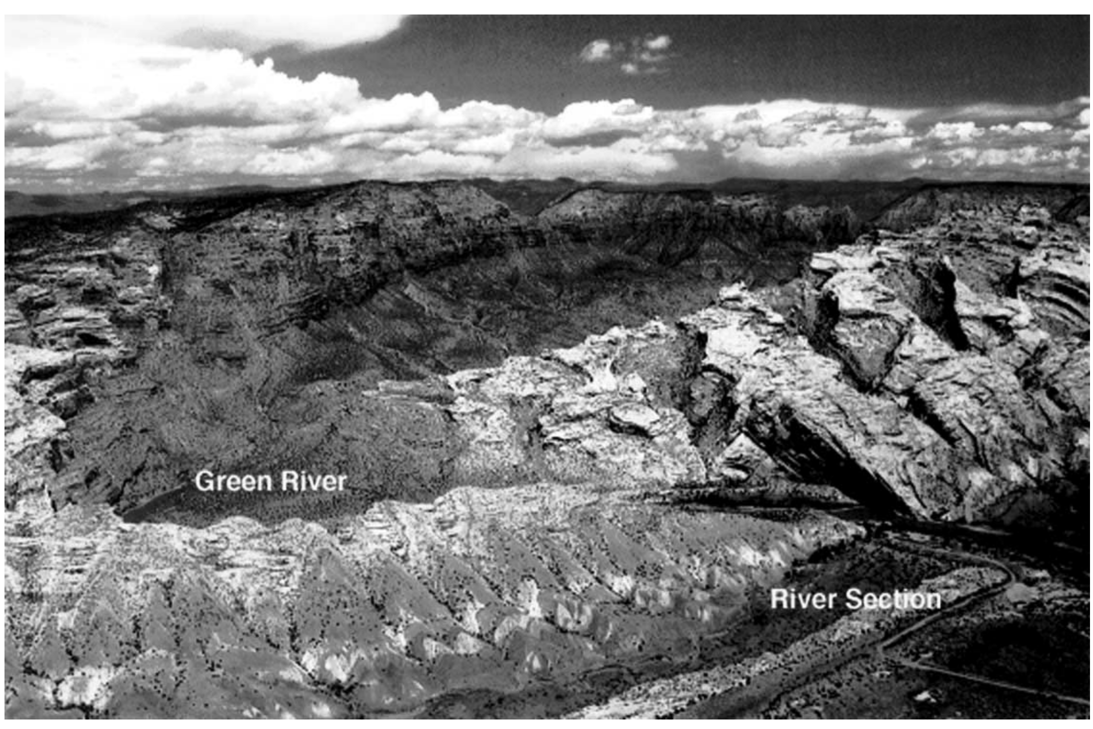

Fig. 3. Photo illustrating drape folding of the Split Mountain anticline. View is indicated by eye icon looking to the NE in Fig. 2.

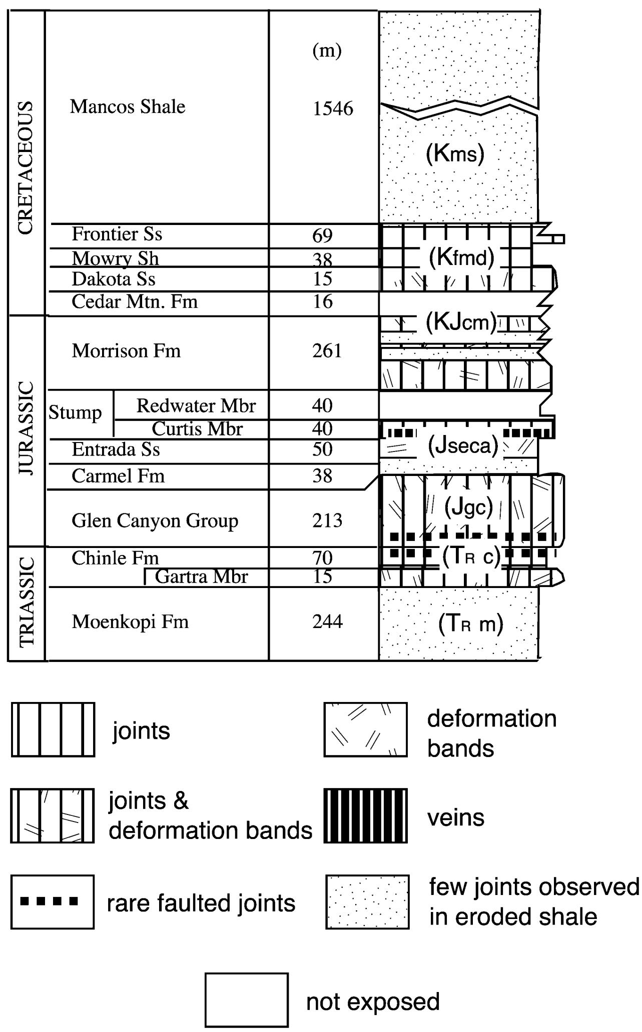

Fig. 4. Generalized mechanical stratigraphy depicting fracturing styles observed in the Mesozoic clastic section around Split Mountain Anticline. Unit thicknesses are in meters. Stratigraphic section adapted from Untermann and Untermann (1949, 1955) and Hintze (1988).

field in which fractures affect the efficiency of tertiary recovery (Narr, 1998).

The Split Mountain anticline is a manifestation of late Mesozoic to early Tertiary compression within the Cordilleran region (e.g. Hintze, 1988). Timing of Cordilleran compressional events is dated by periods of clastic sedimentation (Fig. 4). Deposition in the latter part of the Mesozoic was influenced by the emplacement of major thrust sheets to the west. By the late Jurassic, synorogenic clastics of the Nevadan Orogeny were shed eastward over Utah (Peterson, 1986; Peterson and Turner-Peterson, 1987; Allmendinger, 1992). The major thrusting of the Sevier Orogeny began with initial uplifts along the Paris–Willard thrust system in Idaho, Utah, and Wyoming in earliest Cretaceous time (Armstrong, 1968; Wiltschko and Dorr, 1983). Episodic uplift caused further clastic sedimentation in the form of the sandstones of the Dakota and lower Frontier Formations, units that also contain well developed joint sets.

Initial Laramide uplift in the vicinity of Split Mountain occurred in the western Uinta Mountains along the North Flank and Uinta thrusts in the Late Maastrichtian and continued along these faults into the Paleocene (Bradley, 1995). Uplift progressed into the central and eastern Uinta Mountains in the Early and Middle Eocene along the north-vergent Henry's Fork and Spark's faults, and along the south-vergent Uinta Basin Boundary Thrust system (Hansen, 1984, 1986; Bradley, 1995). Synorogenic sediments of the Fort Union Formation and Wasatch Group were shed from the rising Uinta Mountains and surrounding Laramide uplifts and deposited into the Green River, Piceance, and Uinta Basins. The formation of the Split Mountain anticline and correlative structures to the southeast took place at this time (Fig. 1). Fault-slip analysis suggests that detachment and eastward translation of the Uinta block may have been due to impingement of the Sevier thrusts from the west (Gregson and Erslev, 1997). Laramide uplifts in the surrounding basins include the Grand Hogback monocline, the Axial, Cherokee, and Douglas Creek arches, and the Uncompahgre, Sawatch, White River, and Rock Springs uplifts. The close of the Laramide orogeny in the eastern Uintas coincided with the end of deposition of the youngest Eocene sediments (Hansen, 1984).

The exact relationship between the Split Mountain anticline and basement faulting is unknown. The Teepee anticline at Dinosaur National Monument is interpreted as a interference structure without basement involvement (Novoa et al., 1998). However, Split Mountain is a larger structure and not of the same scale as either the Teepee anticline or other typical interference folds (Wayne Narr and Don Medwedeff, personal communication, 2001). Split Mountain and the larger Uinta arch parallel the trend of the Proterozoic-aged trough filled with an 8–11-km-thick section of the Uinta Mountain Group (Hansen, 1986; Stone, 1993). Proterozoic basement faults were tectonically inverted as indicated by the preservation of the Uinta Mountain Group in the hanging walls of Laramide faults in the Axial, Beaver Creek, and Rangely anticlines but not in the footwalls (Morel et al., 1986; Richard, 1986; Stone, 1986). The general consensus is that Split Mountain is the manifestation of an inverted Precambrian normal fault lifting both the Uinta Mountain Group and the overlying cover into a large N–S bend over an E–W axis (Gregson and Erslev, 1997; Wayne Narr and Don Medwedeff, personal communication, 2001).

3. Structural data from Split Mountain anticline

Fracture data from the Split Mountain anticline were collected at both scanline and transect stations. The highest quality, best-exposed outcrops were reserved for scanline

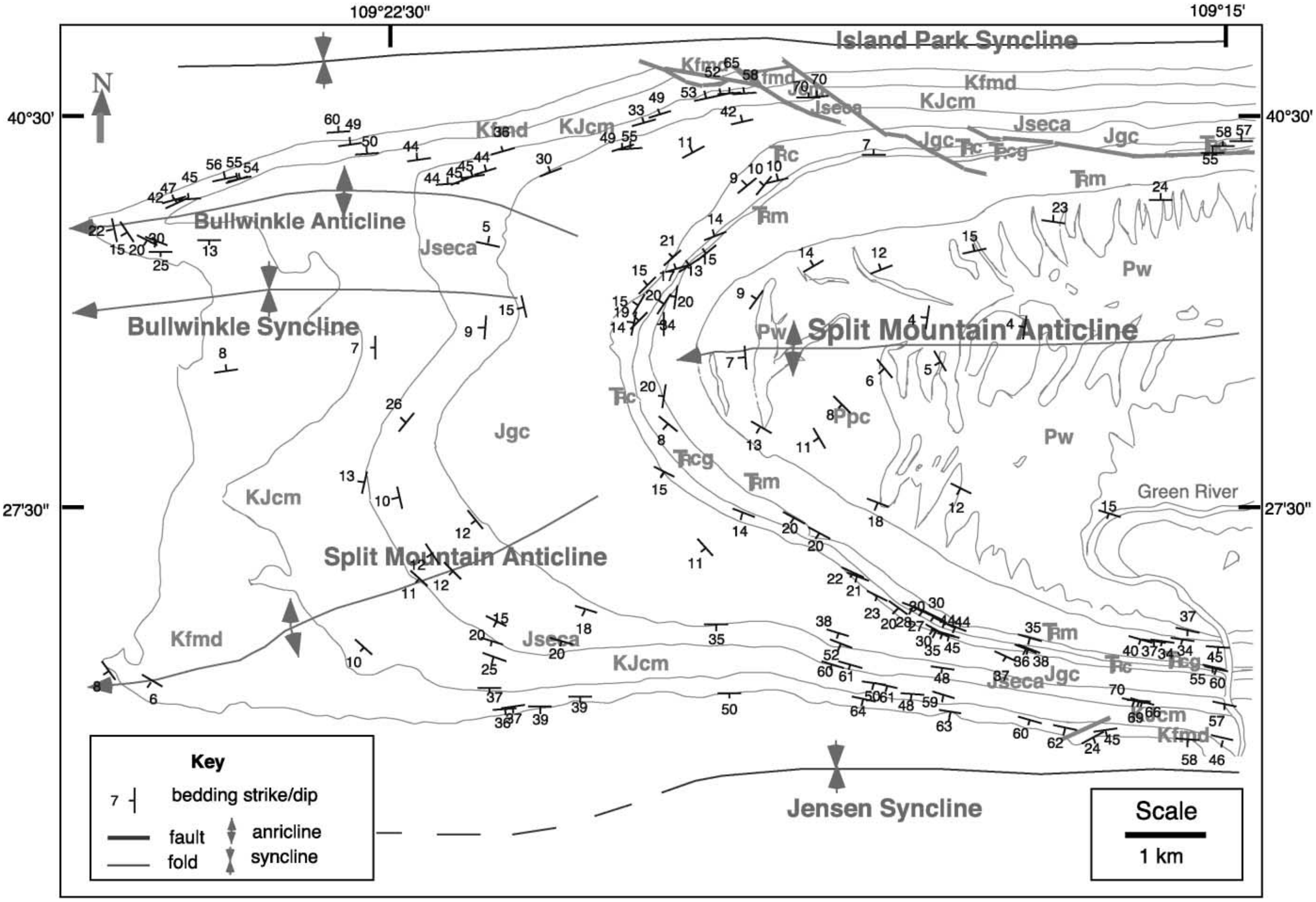

Fig. 5. Average bedding attitudes around the Split Mountain and Bullwinkle anticlines. Attitudes include those measured by the authors and others taken from previous published maps of the area. Geologic map adapted from Doelling and Graham (1972), Rowley et al. (1979) and Rowley and Hansen (1979). Lithologic map symbols are as listed in the caption of Fig. 2.

surveys, which were performed using techniques described by Priest and Hudson (1976), La Pointe and Hudson (1985), and Narr and Suppe (1991). A transect station is an outcrop of insufficient quality for a full scanline survey but of sufficient quality to permit measurement and characterization of a few joints. Transect stations interspersed between scanline surveys allowed for additional outcrop coverage around Split Mountain. Fracturing styles, predominant joint sets, joint orientation, unequivocal abutting relationships, bedding orientation, lithology, and mechanical bed thickness were also recorded at each scanline survey and transect station.

A previous study of Split Mountain collected heterogeneous samples of fault-slip data near major faults and folds (i.e. Gregson and Erslev, 1997). Our sampling focused on unfaulted sections and, in particular, those units with well developed joint sets. However, some units in these 'unfaulted' sections contained a significant number of deformation bands and/or rare faulted joints (Fig. 4). We did not run scan lines in those units in which deformation bands were the most common brittle fracture.

3.1. Mechanical stratigraphy

The Mesozoic clastic rocks around Split Mountain anticline exhibit a style of brittle fracture that varies with lithology (fracture partitioning; Gross, 1995), in this case dependent upon porosity. Well-cemented, fine- to medium-grained sandstone beds and shale beds deform by jointing (e.g. Pollard and Aydin, 1988), whereas more porous sandstone with beds generally thicker than 2 m, deform by local cataclasis along deformation bands steeply inclined relative to bedding (e.g. Aydin, 1978; Antonellini and Aydin, 1995; Davis et al., 1999). Systematic joints are found in the indurated, competent beds of the Frontier, Morrison, and Chinle Formations as well as beds in the Glen Canyon Group, the Curtis Member, and the Mowry Shale (Fig. 4). In contrast, the more porous cross-bedded sandstones of the Frontier, Dakota and Entrada Formations, the Glen Canyon Group and the poorly-cemented conglomerates of the Gartra Member of the Chinle Formation display steeply dipping, anastomosing deformation bands and fewer joints. This study focuses exclusively on joints.

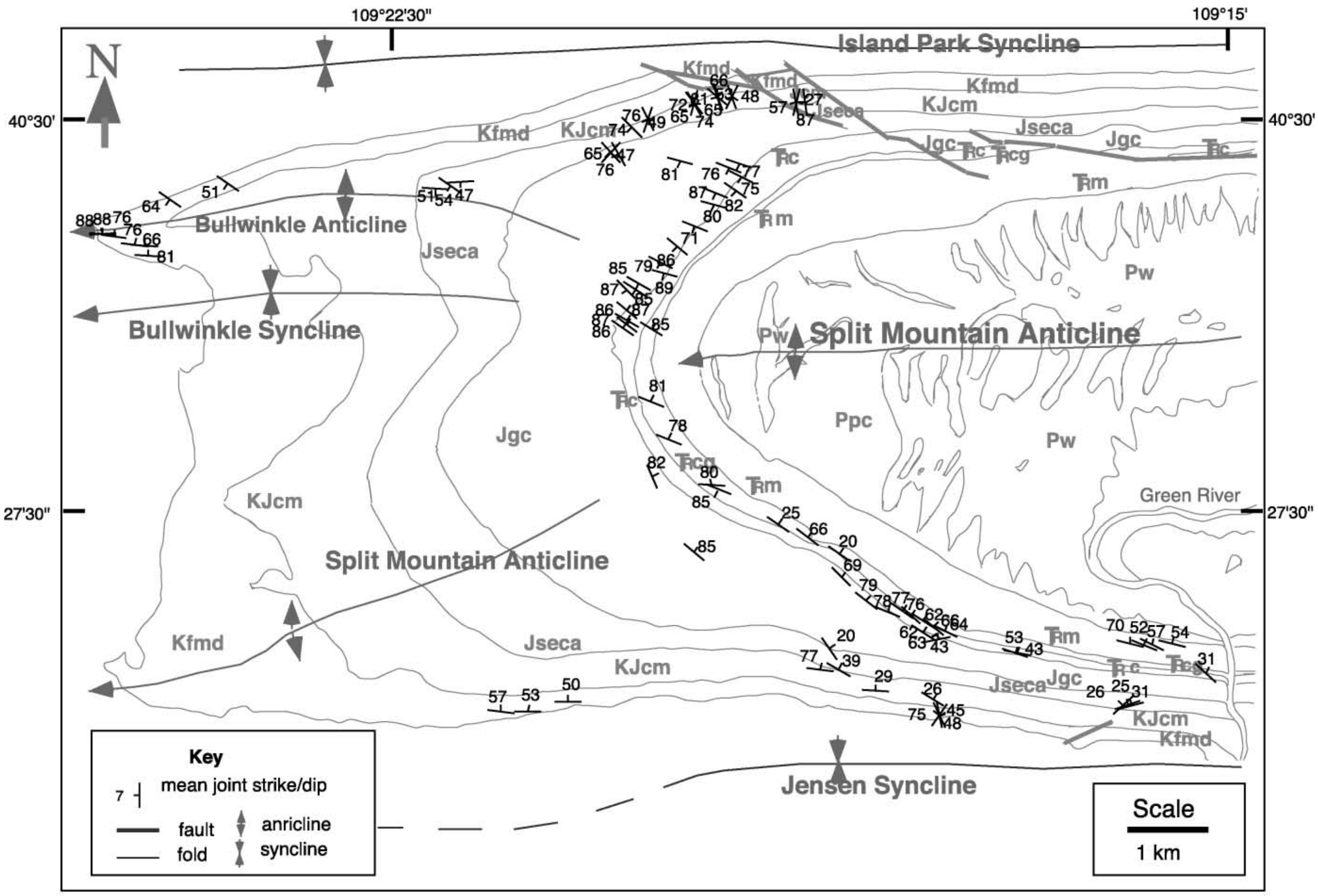

Fig. 6. Systematic joint orientations about Split Mountain. The attitude of the mean joint plane is plotted for each station. See Fig. 4 for a description of geological map symbols. Lithologic map symbols are as listed in the caption of Fig. 2.

In addition to joints and deformation bands, some rocks contain veins and other units are unjointed. Faulted joints are far less common. Because of the large variation in brittle behavior at Split Mountain, we constructed a mechanical stratigraphy (e.g. Corbett et al., 1987; Gross et al., 1997b) that distinguishes among six brittle lithologies based on the manner by which each unit fractures (Fig. 4). Our mechanical stratigraphy includes units with joints (in some cases these are faulted joints), units with deformation bands, units with both joint and deformation bands, units with veins, and shales with very few joints (Silliphant, 1998). As determined by this study, the units containing the best-developed joint sets are the relatively competent beds, including sandstones of the Frontier Formation and sandstones and siltstones of the Glen Canyon Group and the Chinle Formation. Joints showing evidence of shear offset appear only in the Glen Canyon Group and at the top of the Chinle Formation (Wilkins et al., 2001).

3.2. Bedding attitude about Split Mountain

Split Mountain anticline is a west-plunging fold with a broad, gently-folded crest bounded by two flexed hinges with steep flanks (Figs. 2 and 5). Dips for Mesozoic rocks on the exposed flanks of the fold range up to 74°N on the north flank and up to 80°S on the south flank. The fold axis of Split Mountain bifurcates as it plunges to the west. The Bullwinkle anticline, the smaller, more northern portion of the nose of Split Mountain anticline, trends slightly south of west and dips up to 60° on the north limb and up to 30° on the south limb.

3.3. Joint orientation

Scanline data on systematic joints come from several formations, with the best distribution of high quality outcrops found in the Chinle Formation and the Glen Canyon Group around Split Mountain and the Frontier Formation around the Bullwinkle anticline. A vector-mean pole was calculated from the raw orientation data for each scanline and plotted as a dip and strike symbol (Fig. 6). The average vector-mean pole and associated dispersion statistics were also calculated for these rock units (Fig. 7).

A cone of confidence indicates the angular distance from the statistically averaged vector-mean pole within which the true average vector-mean pole for each brittle lithology is found to a certain level of confidence (e.g. Fisher, 1953). The size of a cone of confidence is a measure of the spatial

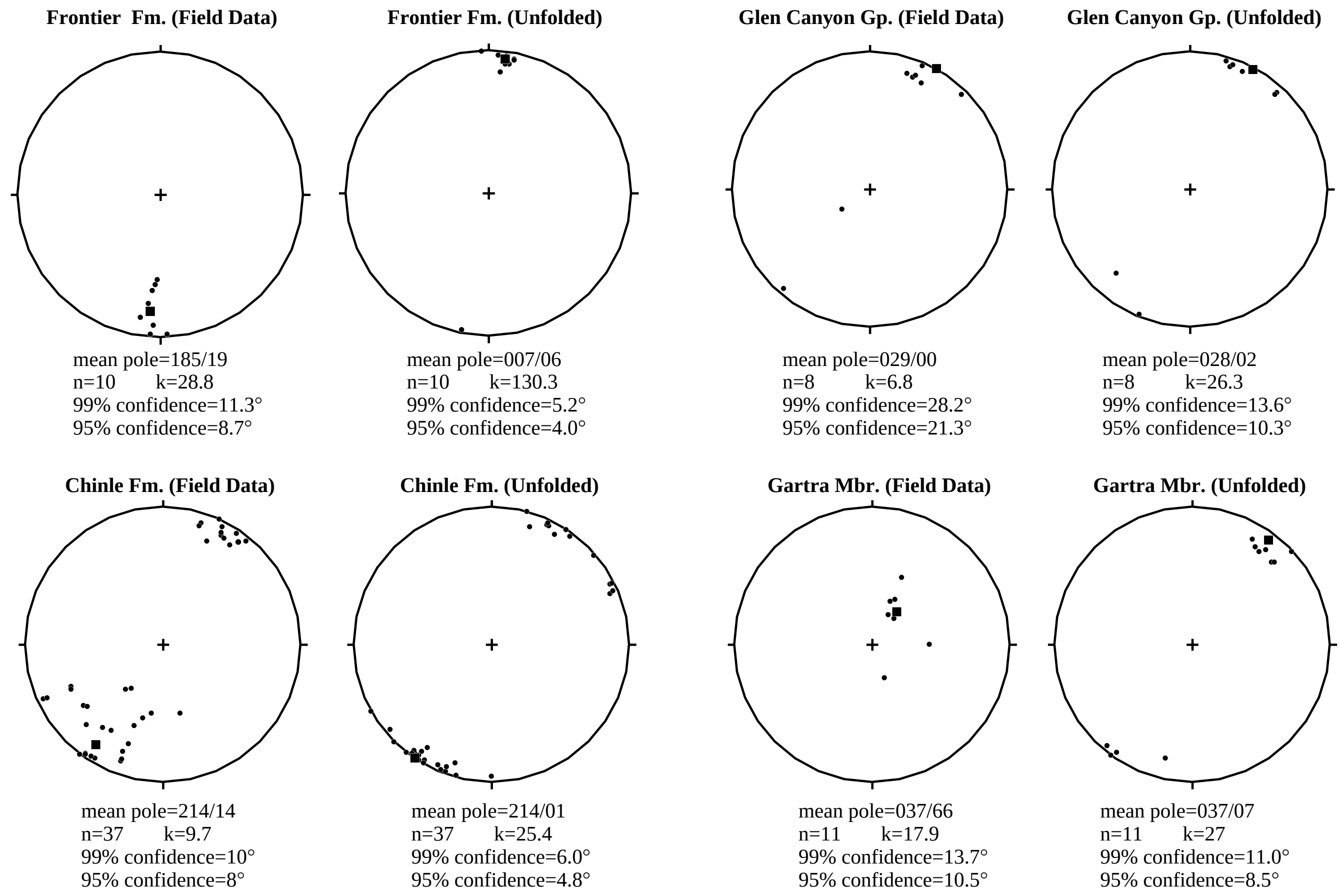

Fig. 7. Lower hemisphere equal area projections of joint orientations as measured in the field and after the host beds were rotated to horizontal. Each data point represents the mean pole from one scanline. Each solid square is the mean pole for the stereoplot. n = number of data. k = McElhinney (1964) precision parameter.

dispersion of orientation data. The mean in situ strike of systematic joint sets and the 95% cone of confidence (α_{95}) for average vector-mean poles for the four joint-bearing rock units combining all stations on both limbs (excluding the Josie's Ranch section) are 275° ($\alpha_{95} = 8.7°$) for the Frontier Formation, 299° ($\alpha_{95} = 21.3°$) for the Glen Canyon Group, 304° ($\alpha_{95} = 8°$) for siltstone beds within the Chinle Formation, and 307° ($\alpha_{95} = 10.5°$) for the Gartra Member of the Chinle Formation. Along the south flank of Split Mountain, the mean azimuths for systematic joints and their dispersion in the Morrison and Moenkopi Formations are 259° ($\alpha_{95} = 27.6°$) and 288° ($\alpha_{95} = 11.8°$), respectively.

3.4. Faulted joints

Joints showing evidence of shear offset appear only in the Glen Canyon Group and at the top of the Chinle Formation, exclusively in the Josie's Ranch section (Fig. 2). The mean orientation of these joints is 295° 62°N with the northern hanging wall down thrown (Wilkins et al., 2001). Striations on this joint set are steeply plunging, indicating normal slip movement. Pinnate joints and wing cracks appear near the tips of these faulted joints (Wilkins et al., 2001). Where present near the bottom of faulted joints, the pinnate joints are located in the footwall and where present near the top of faulted joints, the pinnate joints are located in the hanging wall.

4. Data analysis

The strike of the primary joint set in outcrops of the Glen Canyon Group, Chinle Formation, Gartra Member, and the Moenkopi Formation about Split Mountain is not fold axis-parallel (Fig. 6). Therefore, we consider the possibility that this is a transected joint set that predates folding altogether. Although joints of the Frontier Formation about Split Mountain are transected as well, some joints in the Frontier Formation about the Bullwinkle Anticline and the Morrison Formation about Split Mountain are axis parallel and, hence, are not transected.

If the primary joint set post-dates folding and is controlled by a regional stress field of vertical and horizontal principal stresses, it will have the same attitude on both limbs of the fold, and will be non-orthogonal to bedding when bedding has a significant dip (e.g. Hancock

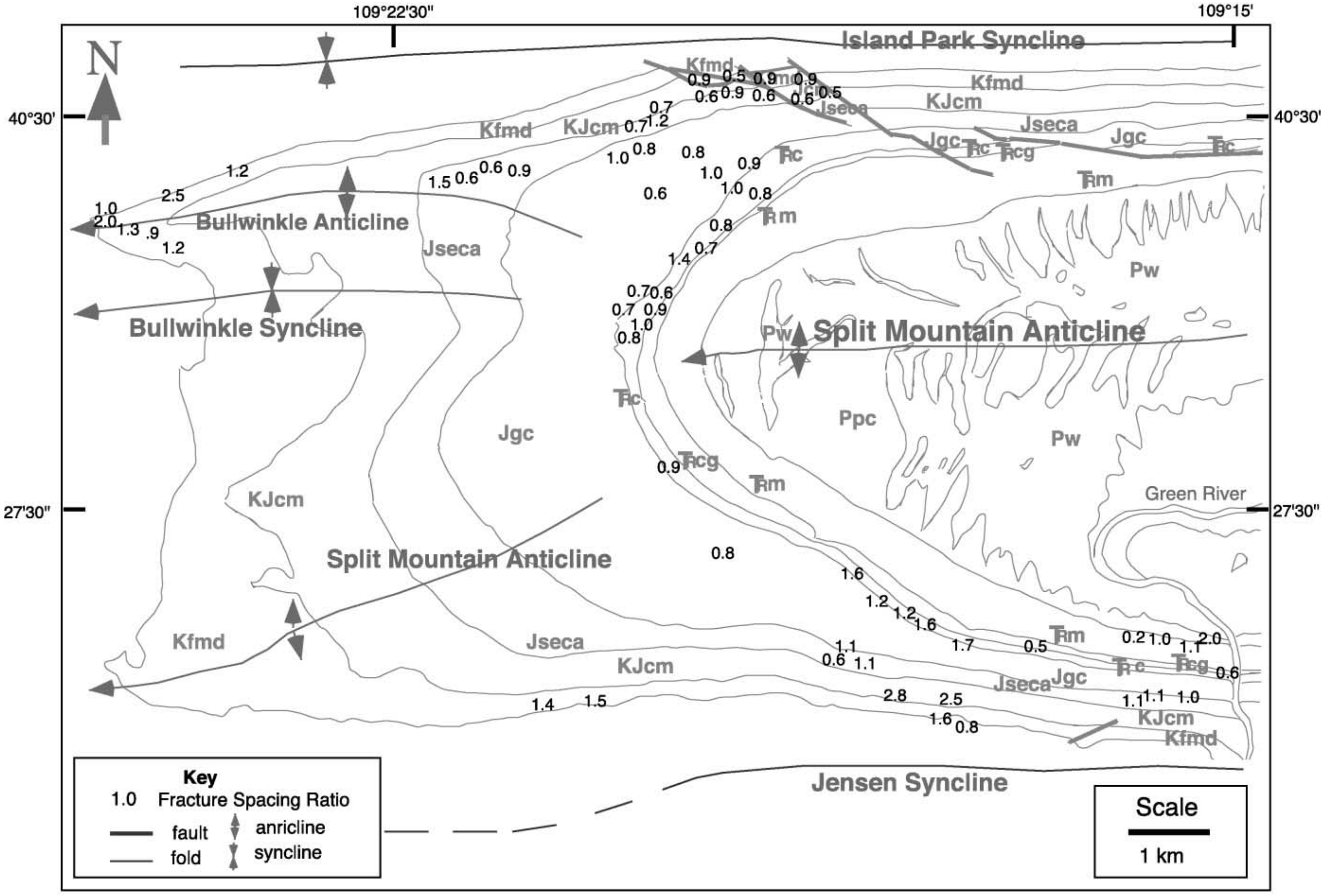

Fig. 8. FSR values calculated from scanlines about Split Mountain. See Fig. 4 for a description of geological map symbols. If multiple scanlines were taken in a single bed, the average FSR value for that location is plotted on the base map. Lithologic map symbols are as listed in the caption of Fig. 2.

and Engelder, 1989). Post-fold jointing that reflects a local, inhomogeneous stress field is unlikely to constitute a systematic set throughout the fold. To test for a transected joint set, we collated joint data from the four rock units with the largest number of scan lines and subjected sets of poles to a fold test similar to that used in paleomagnetic studies. The idea is that a regional, pre-fold joint set forms orthogonal to bedding and is subsequently rotated along with the fold so that it remains orthogonal to bedding.

4.1. The 'pre-fold' joint orientation

The first step in testing for transected joints is to restore bedding to horizontal. The host bed for each scanline survey was rotated back to horizontal, its 'pre-fold' orientation, and the vector-mean pole to the primary joint set within the host bed was rotated through the same angle. Each rotation operation has two steps. First, the trend and plunge of the appropriate fold axis (i.e. Split Mountain or Bullwinkle anticline) was rotated to horizontal and then the bedding plane was brought to horizontal by rotating it around the horizontal fold axis through an angle equal to the dip of the bed. Pi-diagrams were constructed from bedding poles around the nose of each fold to determine the trend and plunge of their respective fold axes: 272°/12° for Split Mountain anticline and 265°/10° for Bullwinkle anticline. These data were used to determine the two rotation angles to bring bedding and the vector-mean pole to joints to horizontal for each scanline.

The vector-mean pole to the rotated systematic joints for each scanline survey corresponds to a 'pre-fold' azimuth of 277° (Frontier Formation), 298° (Glen Canyon Group), 304° (Chinle Formation), and 307° (Gartra Member) (Fig. 7). Vector-mean poles for joints in the Chinle Formation and Glen Canyon Groups indicate joints essentially normal to bedding, whereas vector-mean poles for the Gartra Member of the Chinle Formation and the Frontier Formation dip 83° and 84°, respectively, relative to horizontal bedding. The angle between the average fold axis at Split Mountain (i.e. E–W) and the WNW-striking systematic joint set within three of the four units is about 30° (Fig. 6). Joints in the Frontier Formation are subparallel to the fold axis and are not part of the WNW-striking joint set in the Chinle Formation, Gartra Member of the Chinle Formation, and the Glen Canyon Group.

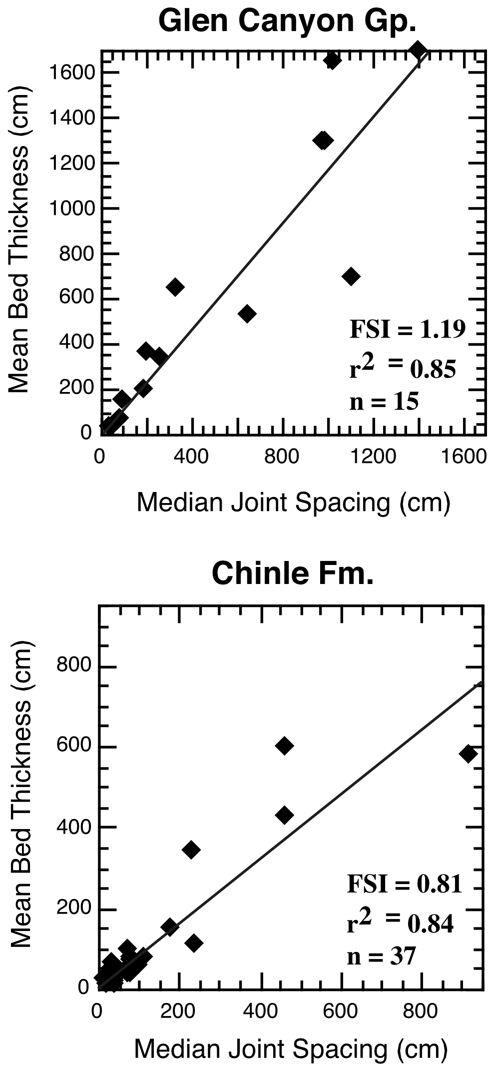

Fig. 9. FSI plots for the Glen Canyon Group and the Chinle Formation about Split Mountain.

4.2. Fold test

By comparing the dispersion of the vector-mean poles in their 'unfolded' orientation with the dispersion of vector-mean poles to joints in their present orientation, we can determine admissibility of the hypothesis that initial joint propagation predated folding. We do so by drawing upon the principle of the paleomagnetic fold test: "magnetism directions older than the folding phase must be statistically better clustered (oriented in a preferred direction) before their bedding attitudes are altered by tilting" (McElhinny, 1964). By the same logic, if the fold transected systematic joints, the dispersion of joint orientations measured around the fold should be significantly less in the unfolded position (after post-tilt correction) than in the folded position.

Statistical significance is measured by the variance in dispersion of poles to joints observed before and after folding as explained in Fisher (1953) and McElhinny (1964). On applying the fold test we conclude that the hypothesis for pre-folding propagation of WNW jointing is admissible because the data are statistically significant at the 99% confidence level.

There is a caveat to this conclusion. If a systematic joint set developed in response to tangential longitudinal strain, and hence is syn-folding, that set could actually become better clustered after beds are unfolded. This is because the joints would be normal to bedding (and strike parallel to fold axis trend), and thus their dips would not be uniform in the present folded state. This may give the incorrect perception that the joint set is pre-folding (i.e. if based solely on the fold test). However, one criterion for tangential longitudinal strain-related joints is that the orientation of the great circle girdle to joint poles would align with either the local fold axes or maximum curvature at some time during fold development. In fact, the poles to the girdles for joints from the Chinle Formation, Gartra Member, and Glen Canyon Group do not align with the fold axis. Likewise, they are so pervasive that they did not develop in response to a local maximum curvature.

4.3. Joint spacing

Joint spacing is one measure of joint density, the parameter that several geologists have correlated with fold curvature (i.e. Lisle, 1994; Hennings et al., 2000). The average spacing between systematic joints in competent beds of interlayered sedimentary rocks is often proportional to the bed thickness (Ladeira and Price, 1981; Narr and Suppe, 1991; Gross et al., 1995; Engelder et al., 1997). Other parameters also affect joint spacing: elastic properties and fracture toughness of the rock, initial flaw size, thickness of the incompetent units, and propagation mechanism (e.g. Fischer et al., 1995; Gross et al., 1995; Ji and Saruwatari, 1998; Bai and Pollard, 2000). Joint spacing is normalized according to bed thickness so that spacing from single beds of different thickness may be compared in a meaningful manner. The normalized parameter for joint spacing in individual beds, the inverse of median-spacing/thickness, is called the fracture spacing ratio (e.g. Gross, 1993; Gross et al., 1997a). When characterizing the spacing data from several beds within a common rock unit, normalized joint spacing is represented by the slope of the linear regression of bed thickness vs. median fracture spacing (i.e. the fracture spacing index of Narr and Suppe (1991)).

The typical fracture spacing ratio for scanline surveys around Split Mountain anticline ranges from 0.6 to 1.6 (Fig. 8). A fracture spacing index was calculated for the Glen Canyon Group throughout Split Mountain and Chinle Formation on the northwest flank of Split Mountain (Fig. 9). Each datum on the fracture spacing index plots is from a scanline survey containing at least nine systematic joints (seven in the case of two beds exceeding 4 m in thickness). The fracture spacing index for the WNW joint set in the Glen Canyon Group (= 1.19) is higher than that found for the WNW joint set in the Chinle Formation (= 0.81). We do

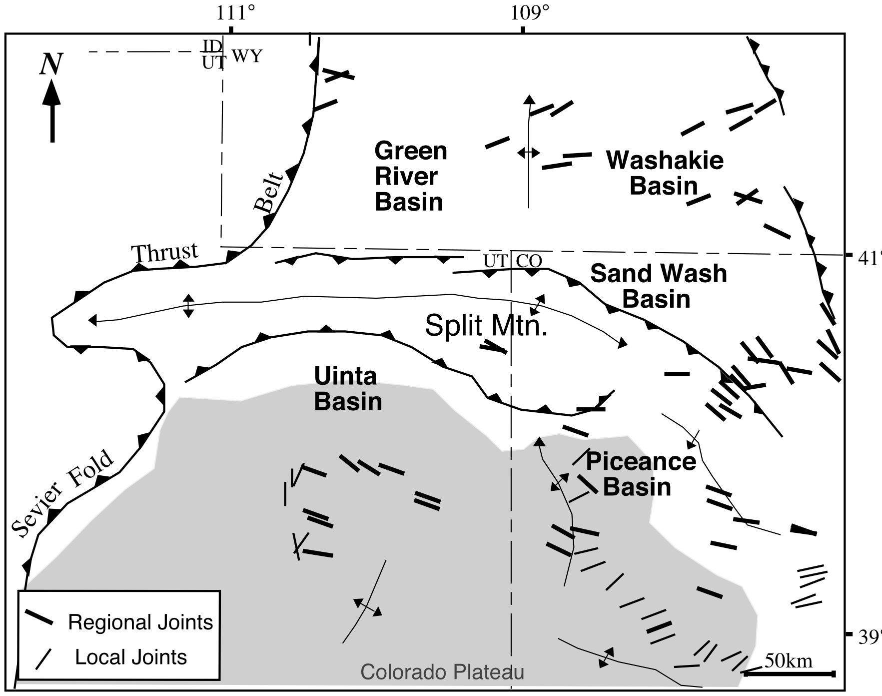

Fig. 10. Orientation of regional joints and coal cleats in the basins surrounding Split Mountain anticline. Data compiled from Harper (1964), Dula (1981), Hucka (1991), Grout and Verbeek (1992a,b), Laubach et al. (1992a,b), Tyler et al. (1992a,b), Lorenz and Hill (1994) and Narr (1998).

not obtain a reasonable fit for a fracture spacing index line from Chinle data taken on the south flank of Split Mountain.

The lower fracture spacing index for the Chinle Formation is due, in large part, to inclusion of data from the Northwest Section (Figs. 1 and 7). Joint spacing in the Chinle on the south flank of Split Mountain, particularly the Quarry Section, show several fracture spacing ratios >1.0. To test for a statistical difference between joint spacing in the Chinle Formation of the Northwest Section and spacing on the south flank of Split Mountain, we apply Student's *t*-test (Engelder et al., 1997). We test whether the mean fracture spacing ratio of the Northwest section of Split Mountain and the mean fracture spacing ratio of the south flank (Quarry and River sections) represent the same population. The null hypothesis is not rejected, indicating that the two data sets come from the same discrete population at the 95% confidence level. Therefore, we proceed with the interpretation that fracture density does not vary significantly with structural position and that this fracture density was inherited from the time of joint development prior to folding.

5. Discussion

5.1. A Pre-Laramide regional joint set

Our hypothesis is that the predominant WNW-striking joint set within the Glen Canyon Group (298°), the Chinle Formation (304°), and the Gartra Member of the Chinle Formation (306°) on both flanks of the Split Mountain anticline predates folding. A fold test indicates that this hypothesis cannot be rejected at the 95% confidence level. If our hypothesis is true, the WNW joints at Split Mountain are likely to constitute part of a regional set that appears elsewhere. Indeed, there is plenty of evidence for such a set beyond the immediate vicinity of Split Mountain.

Pre-Laramide, WNW-striking systematic joint sets are found in Cretaceous or older rocks in the Piceance Basin to the east (Verbeek and Grout, 1997), the Uinta Basin to the south (Verbeek and Grout, 1992), and the southeastern Sand Wash Basin (Fig. 10). At Rangely anticline, Colorado, vertical joints striking WNW–W appear in both the Permian Weber Sandstone and the Cretaceous Castlegate Formation (Narr, 1998). Joints trending between 275 and 290° in Upper Cretaceous and older rocks on the Laramide Grand Hogback monocline, Colorado and White River uplift, Colorado are interpreted to pre-date folding (Harper, 1964; Murray, 1967; Dula, 1981; Lorenz et al., 1991; Lorenz, 1995; Tremain and Tyler, 1997; Narr, 1998). Joints in cores taken from the MWX and SCHT wells, Colorado also trend between 276 and 279° in the Upper Cretaceous Mesa Verde Group (Lorenz and Finley, 1991; Lorenz and Hill, 1994). WNW–NW-trending coal cleats (275–280° to 315–355°) in Upper Cretaceous to Lower Tertiary rocks exist throughout the southeastern Sand Wash Basin (Tyler and Tremain, 1993). North of the Uinta Mountains in the Green River Basin, E- and ENE-striking, pre-Laramide joints are documented along the western margin, in core from the center of the basin, and on the Rock Springs uplift (Laubach, 1992;

Laubach and Lorenz, 1992; Tyler et al., 1992a,b; Lorenz, 1995). Tertiary rocks also carry joints of this orientation. Coal cleats in the Tertiary Price Formation in the south-central Uinta Basin strike 295–320° and dip perpendicular to bedding (Hucka, 1991).

At each location mentioned above (including Split Mountain), the pre-Laramide systematic joint sets and/or face cleat sets strike perpendicular or sub-perpendicular to the arcuate trend of the Sevier Fold and Thrust belt (Fig. 10). Since the strike of joints and cleats define the trajectory of the maximum horizontal stress cratonward from the Sevier belt, Laubach (1992) suggests that they propagated during the period of Cretaceous Sevier and Early Tertiary foreland compression. Similar regional joint patterns reach into the forelands of the Ouachita and Appalachian Mountains (Melton, 1929; Nickelsen and Hough, 1967; Engelder and Geiser, 1980). The presence of WNW-striking joints in each of the basins in the vicinity of Split Mountain further strengthens our conviction that joints at Split Mountain were transected by Laramide folding.

5.2. Constraints on stress during folding: minor faulting

The 22 samples that Gregson and Erslev (1997) collected for fault inversion show a very complex pattern that indicates a N–S to NNW–SSE compression. This is the orientation of a regional compression that forced reactivation of basement faults over which Split Mountain is draped. Such a compression is inconsistent with the down-dip slip on joints of Split Mountain. Apparently, the folding of sizable panels of rock at Split Mountain generated a local stress that favored neither pervasive frictional slip on existing joints nor the formation of new joints. We conclude that basement stress did not superimpose on the bending stress developed in draped cover rock, a lesson gleaned from the analysis of jointing at other Laramide folds as well (e.g. Engelder et al., 1997; Fischer and Wilkerson, 2000; Maschmeyer and Cooke, 2000). The literature documents many examples of extension within folds when the remote stress favors regional shortening (i.e. Srivastava and Engelder, 1990; Lemiszki et al., 1994).

5.3. Constraints on stress orientation during folding: down-dip slip on joints

The state of stress in the limb of a fold is constrained by the presence of transected joints that show no evidence of slip. Our goal is to constrain the stress in large panels of folded rock by means of a slip criterion for faulted joints. The simplest explanation for lack of slip on most transected joints is that they were never subject to a shear stress despite being tilted 30° or more. If bending was accompanied by tangential–longitudinal strain, local stresses may have been forced to rotate and thus remain orthogonal to bedding (e.g. Price and Cosgrove, 1990; Lemiszki et al., 1994). In this case, transected joints remained orthogonal to principal stresses and were never subject to a resolved shear stress.

While the overwhelming majority of the transected joints were locked without slipping during folding, Wilkins et al. (2001) observe that WNW joints with a dip of 62° in the Josie's Ranch section slipped (Fig. 2). This means that some transected joints were carried into a plane of higher resolved shear stress by the tilting of beds during Laramide folding. Down-dip slip on these transected joints indicates that the local stresses did not rotate to remain orthogonal to bedding during folding. Lack of an appreciable stress rotation is attributed to the weight of overburden. Even if a tangential longitudinal strain mechanism was active during folding at Split Mountain, the weight of overburden would have superimposed a large vertical component of stress on the local bending stress to restrict the rotational tilting of a local vertical principal stress to a few degrees off vertical. Because of this superposition, pre-folding joints tilted more than a few degrees from vertical were undoubtedly subject to a shear stress. The resolved shear stress was, however, not large enough to overcome the locking mechanism on most joints until these joints reached dips of approximately 62°. Then down-slip slip took place.

Down-dip slip indicates that a cross section normal to the fold axis (i.e. *a*–*c* plane; Hancock, 1985) of the Split Mountain anticline contains the vertical principal stress, S_v (i.e. σ_1), and the minimum horizontal principal stress, S_h, with $S_v > S_h$ as indicated by down-dip slip on faulted joints (Wilkins et al., 2001). The intermediate principal stress would have been the maximum horizontal stress, S_H, parallel to the fold axis or normal to the local dip direction. This is the stress state consistent with extensional tectonics where gravity loading is responsible for the maximum principal stress. In the vicinity of the River and Quarry sections the *a*–*c* plane was normal to the E–N axes of both Split Mountain anticline and Jensen syncline (Fig. 2). Near the Josie's Ranch section, the *a*–*c* plane (i.e. NNE–SSW) is normal to the Jensen syncline as it changes trend to the southeast (Fig. 2). As will be shown, this orientation restricts us to the most conservative estimate for stress difference, σ_d.

5.4. Constraints on stress magnitude during folding: down-dip slip on joints

Two rock properties serve to lock a joint subject to a shear stress and prevent slippage: (1) fracture toughness of the rock, and (2) the frictional strength of the joint. If a joint is open and not in frictional contact, shear stress will cause an elastic displacement parallel to the plane of the joint (Pollard and Segall, 1987). Such displacements are very small and fully recoverable once the shear traction is removed. The joint remains locked unless cracks are driven from the joint tips. Shear stresses above a certain level will drive much larger and possibly irreversible slip accompanying the opening of a crack at each tip of the joint. Such new cracks will occur at an angle to the plane of the pre-existing joint and follow a curved path to form wing cracks (Brace

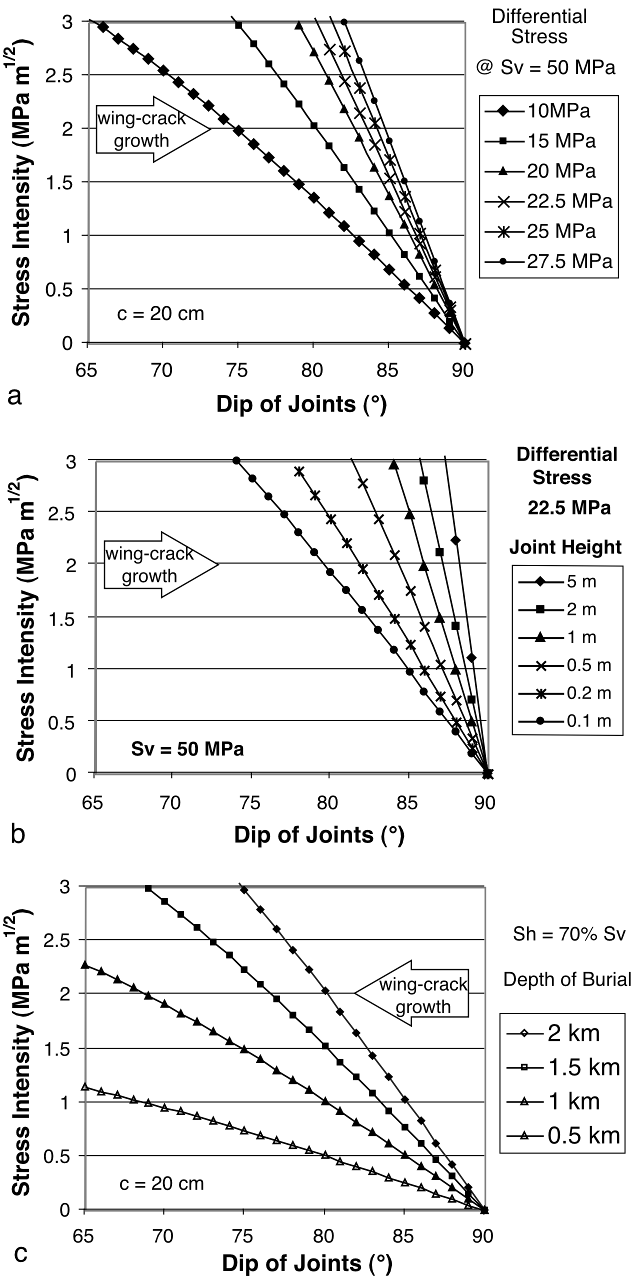

Fig. 11. (a) Stress intensity (K_{II}) as a function of joint dip for beds at 2 km of burial. Curves are for various differential stresses acting on a blade crack of length = 40 cm. (b) Stress intensity as a function of joint dip for beds of various thicknesses at 2 km of burial. (c) Stress intensity as a function of joint dip for beds at a variety of burial depths. The differential stress at each depth is set so that $S_h = 70\%\ S_v$.

and Bombolakis, 1963) or kinks (Cruikshank et al., 1991). A finite shear stress governed by the fracture toughness of the rock is required to initiate the growth of wing cracks and thereby unlock the joint for non-recoverable shear displacement.

Joints may not be open and, in this case, frictional strength of the joint surface may keep the joint locked to prevent slippage. If joint walls are in frictional contact, the resolved shear stress must exceed the joint's frictional strength before the tip of the joint can be loaded to induce the propagation of wing cracks. Even if shear stress is high enough to initiate frictional slip, the fracture toughness of the rock could still act to prevent all but elastic slip. Consequently, for any resolved shear stress, a joint must exceed two strength criteria acting in series (i.e. frictional strength before tensile strength) before the joint will slip. Hence, we can estimate the range of principal stresses required to overcome these locking mechanisms (i.e. friction and fracture toughness), assuming a gravity load keeps the principal stresses approximately vertical and horizontal during folding at Split Mountain. This calculation gives us a conservative estimate for the limit to the differential stress acting on joints during bed tilting at Split Mountain. If the local principal stresses partially rotate with the bedding by a tangential longitudinal strain mechanism, then a larger differential stress would have been required to unlock joints and drive shear displacement.

5.4.1. Locking by fracture toughness

Parameters that allow us to calculate the onset of slip on an open joint include the size of the joint and the fracture toughness of the host rock (Lawn, 1993). Non-elastic slip on an open joint will only occur when the stress intensity at the joint tip, K_{II}, exceeds the fracture toughness, K_{Ic}, of the rock. Initially, we assume that the joint is just barely open (i.e. without frictional strength) but not subject to significant opening mode stress intensity (i.e. $K_I = 0$). K_{II} for a joint normal to bed boundaries varies according to:

$$K_{II} = Y\tau_{xy}\sqrt{\pi c} \tag{1}$$

where $Y = 1$ is the shape factor for a blade crack (i.e. a joint in a sandstone confined between shale layers), τ_{xy} is the shear stress on the plane of the joint, and c is the half length of the joint (i.e. half the thickness of the sandstone layer). Slip will take place if wing cracks propagate from the joint tips and into the bounding layers, usually shale, when $K_{II} > K_{Ic}$ (Ingraffea, 1987). From Eq. (1), we see that stress intensity increases with joint length (i.e. the vertical dimension at Split Mountain) so that tall joints in thicker beds are more likely to slip than short joints in thinner beds. In fact, faulted joints at the Josie's Ranch section commonly have a length >10 m in beds as much as 14 m thick in the Glen Canyon Group (Wilkins et al., 2001).

To calculate the state of stress in the limbs of the Split Mountain anticline we incorporate the overburden load. The local stratigraphic column suggests that tilting of the Chinle Formation and Glen Canyon Group took place under about 2 km of overburden (Fig. 4). Assuming an average density of 2.5 g/cc this gives a total vertical stress ($S_v = 50$ MPa and compressive stress is positive). We will assume a hydrostatic water column for a pore pressure where $P_p = 21$ MPa at 2 km, giving an effective vertical stress, $\bar{S}_v = 29$ MPa.

Assuming vertical and horizontal principal stresses (i.e. the principal stresses do not tilt with bedding), both τ_{xy} and

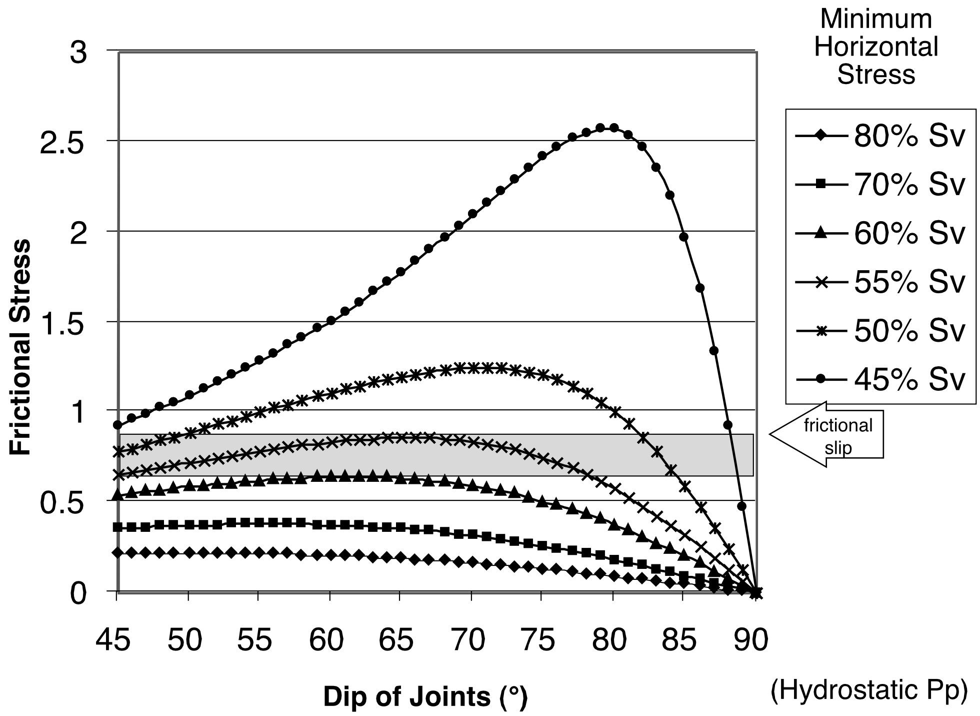

Fig. 12. Frictional stress as a function of joint dip for various ratios of horizontal to vertical stress. Top boundary of the shaded band marks the frictional stress for rocks according to the compilation of Byerlee (1978).

K_{II} increase as beds tilt and carry joints away from a vertical orientation. The example given in Fig. 11a plots K_{II} on a joint in a 40-cm-thick bed (e.g. $c = 20$ cm) subject to several possible differential stresses found at 2 km under hydrostatic pore pressure. Because joints did not propagate during folding, we can reasonably assume that an effective tension was not present during folding. Hence, at a depth of 2 km, the maximum differential stress was on the order of 29 MPa, at which point $\bar{S}_h$ would have been zero. The magnitude of K_{II} depends on both the angle of the joints relative to the plane of the principal stresses and the magnitude of the differential stress, $S_v - S_h$. Vertical joints are in a plane of principal stresses and, therefore, not subject to mode II loading. As beds are tilted by folding, transected joints are subject to an increasing large resolved shear stress. This is seen as an increase in stress intensity with a decreasing dip of the joints (Fig. 11a).

Now, if we assume, for example, that $K_{Ic} = 2$ MPa m$^{1/2}$ and $S_v - S_h = 10$ MPa, a 40-cm-thick bed must rotate about 15° (i.e. the joint dips 75°) before slip takes place by means of wing crack development (Fig. 11a). If $S_v - S_h = 20$ MPa, the same bed must tilt only 8° (i.e. the joint dips 82°) before slip takes place. When $\bar{S}_h = 0$ MPa (i.e. $S_v - S_h = 29$ MPa), a bed ($c = 20$ cm) must tilt only less than 6° before wing cracks will develop on bed-normal joints assuming $K_{Ic} = 2$ MPa m$^{1/2}$. According to Eq. (1), less tilting is required to initiate slip on taller joints in thicker beds (Fig. 11b).

The effect of depth of burial is also of interest. Suppose that we want to understand the amount of bed tilt required for wing crack initiation when $S_h = 70\%\ S_v$. At a depth of 2 km, beds must tilt 10° before slip accompanying wing crack initiation is possible (Fig. 11c). Again we assume that the joint does not have a frictional strength and that $K_{Ic} = 2$ MPa m$^{1/2}$. At a depth of 1 km, beds must tilt more than 20°. This is largely because differential stress has decreased with decreasing depth of burial, a common phenomenon in the crust of the earth (Engelder, 1993). However, we conclude that, in general, if joints at Split Mountain were without a frictional contact, they should have slipped by the time beds tilted to 15°, if $\sigma_d \geqq 10$ MPa (Fig. 11a). Yet, a significantly larger tilt (i.e. 28°) was required before joints were unlocked and slipped.

5.4.2. Locking by frictional strength

So far, our analysis assumes that joints are frictionless. If, in fact, joints are in frictional contact, the shear stress parallel to the joint surface must reach a certain magnitude before static friction is overcome. Only then will the stress intensity at the joint tip increase and induce the growth of wing cracks. The larger the difference between S_v ($=\sigma_1$) and S_h ($=\sigma_3$), the greater the shear stress on the joint. Shear stress can be normalized using the effective normal stress to obtain a dimensionless parameter:

$$\sigma_\mu = \frac{\tau_{xy}}{\sigma_n - P_p} \tag{2}$$

that is independent of burial. If this dimensionless parameter, called frictional stress, exceeds the coefficient of rock friction, then the joint will slip. This frictional stress is also independent of joint size, in contrast to stress

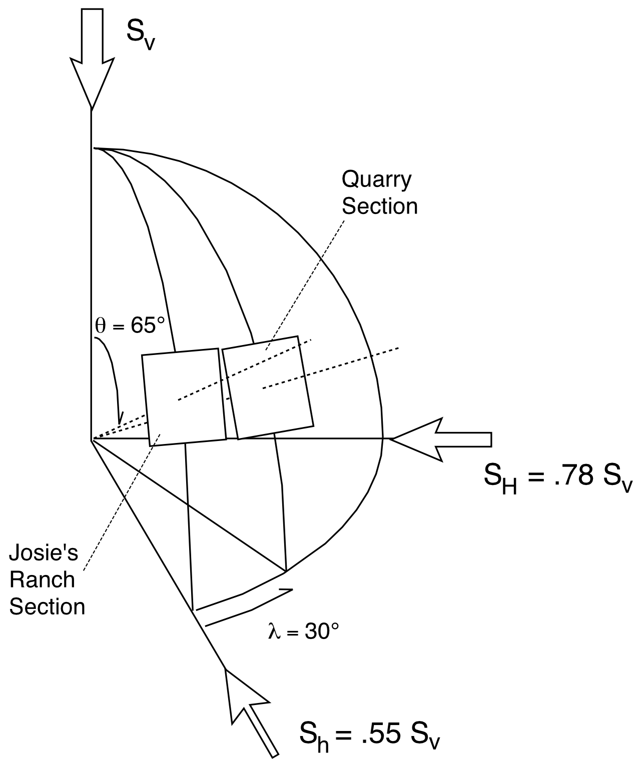

Fig. 13. The orientation of the WNW regional joints relative to a local stress developed during folding. $\theta =$ dip of joints. $\lambda =$ misalignment between strike of joints and local fold axes. While this figure may suggest that the joints of Josie's Ranch have a different orientation from those within the Quarry section, it is actually the principal horizontal stresses that change between these two sections.

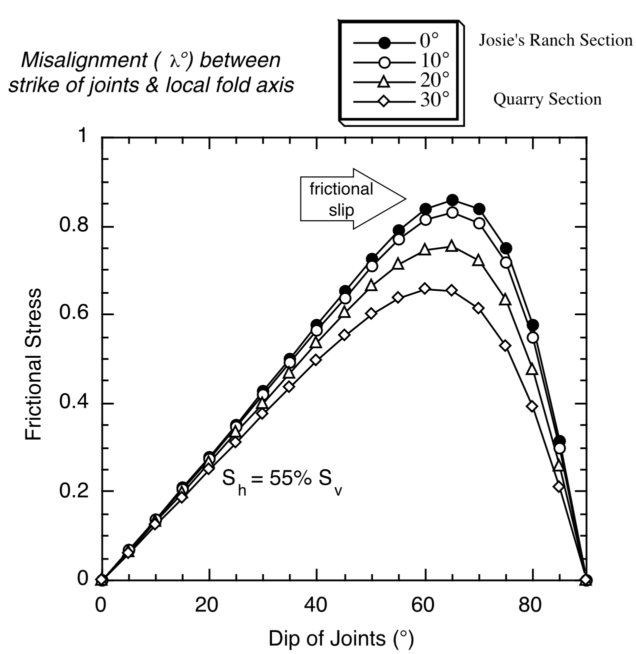

Fig. 14. Frictional stress as a function of joint dip for various misalignments between strike of joints and local fold axes.

intensity which is a function of joint size (Eq. (1)). We can calculate a normalized shear stress (i.e. the frictional stress) on joints as a function of joint dip (Fig. 12). The coefficient of rock friction in the shallow crust is on the order of 0.85 (Byerlee, 1978). If the stress difference is low (i.e. $S_h \geqq 0.6S_v$), the frictional stress does not exceed the coefficient of friction and joints will not slip regardless of the tilt of bedding during folding. Even when frictionless joints have a crack tip stress intensity large enough to drive wing cracks after beds are tilted, there will be no such propagation as long as the joints are locked by friction. For a larger stress difference (i.e. $S_h = 0.55S_v$), frictional stress will have caused frictional slip on joints in beds that were tilted to more than 20°. If the stress difference is larger, slip will occur on joints after less bedding tilt. Once joints slip at a depth of 2 km, the joint-tip stress intensity is high enough to cause wing crack growth on joints in beds as thin as 10 cm (Fig. 11b).

The best examples of faulted joints at Split Mountain are found in the Josie's Ranch section, where beds 1–14 m thick tilt so that the dip of joints is about 62° (Wilkins et al., 2001). At this dip, the joints have just passed through the orientation (i.e. 65°) for highest frictional stress when $S_h = 0.55S_v$ (Fig. 12). Joints of shallower dip are subject to less frictional stress and, indeed, have not slipped. Throughout Split Mountain only those joints in an optimum orientation (≈ 65°) for generating maximum fictional stress have slipped. Because joints in a very restricted range of dips actually slip and because the rock has a frictional strength of $\mu = 0.85$ (i.e. Byerlee, 1978), we can estimate the differential stress within the tilted beds at Split Mountain. We conclude that at a depth of 2 km, the differential stress was 22.5 MPa at a hydrostatic pore pressure.

5.4.3. Locked joints with an optimum dip

At Josie's Ranch where joints are faulted, the *a–c* section is taken normal to the Jensen syncline (Fig. 2). Here, the poles to joints dipping at ($\theta =$) 62° are in the plane defined by σ_1 (S_v) and σ_3 (S_h) (Fig. 13). However, not all joints tilted to the optimum angle (i.e. ≈ 65°) have slipped. There are many such examples in the Quarry and River sections of Split Mountain (Fig. 2). Locked joints with an optimum dip may be explained if we assume that the principal stresses and the *a–c* section are orthogonal to the fold axes in the vicinity of the Quarry Section (i.e. ≈ S_h is approximately N–S). In this case there is a misalignment of ($\lambda \approx$) 30° between the strike of joint planes and the direction of the least horizontal principal stress (Fig. 13). This misalignment has a significant bearing on the frictional stress to which the joints are subjected upon tilting. The normal and shear stresses on dipping joints are given by Jaeger and Cook (1976) as:

$$\sigma_n = \left[\sigma_3\cos^2\lambda + \sigma_2\sin^2\lambda\right]\sin^2\theta + \sigma_1\cos^2\theta \quad (3)$$

$$\tau = \tfrac{1}{2}\left[\sigma_1 - \sigma_2\sin^2\lambda - \sigma_3\cos^2\lambda\right]\sin 2\theta \quad (4)$$

The normal stress on the plane of the joints is somewhat larger and the shear stress is somewhat smaller on the joints in the Quarry section where $\lambda = 30°$. Maximum frictional stress on the plane of joints in the Quarry section is approximately 75% of that achieved in the Josie's Ranch section where the intermediate principal stress was in the plane of bedding (Fig. 14). Consequently, joints in the Quarry section may pass through the orientation of optimum dip without yielding (i.e. slipping).

In summary, most of the pre-fold joints at Split Mountain are not optimally oriented for frictional slip and remained locked during the folding process. Dip alone is not a sufficient criterion for reaching the critical frictional stress but rather the orientation of the joint within a 3-D stress state must be considered. In general, it is the frictional strength of joints, not fracture toughness of rocks, that keeps transected joints locked during tilting by bending.

6. Conclusions

Brittle fracture within the Split Mountain anticline is characterized by jointing in the indurated sandstone and siltstone beds of the Frontier, Morrison, and Chinle Formations, the Glen Canyon Group, the Curtis Member of the Stump Formation, and the Mowry Shale. The most common joint set is a systematic WNW-striking joint set found within the Glen Canyon Group and Chinle Formation on both flanks of the Split Mountain anticline. Evidence suggests that this set was formed prior to folding as part of a later-transected, regional joint set. During formation of the anticline, frictional strength prevented slippage on most joints of this set as beds tilted and the joints were subjected to a larger resolved shear stress. Once fold-related tilting of bedding carried these joints to an optimum dip of 62°, some of the joints in the Glen Canyon were faulted with a down-dip slip of the hanging wall. Down-dip slip on faulted joints reflects an overall horizontal extension as the folded Mesozoic section was bent over reactivated faults in basement. Extension indicates that the stress state during folding was $S_v > S_H > S_h$. Down-dip slip on faulted joints indicate that the lateral constraint (i.e. S_v) was reduced causing an increase in the differential stress. The orientation, both dip and strike, of faulted joints places an important constraint on the stress state in the limbs of the Split Mountain anticline during folding. Hence, using a criterion for frictional slip on faulted joints we conclude that horizontal stress must have decreased to about 55% of the overburden on the indurated sandstone and siltstone beds under 2 km of overburden.

Acknowledgements

We thank the United States Department of the Interior and the National Park Service at Dinosaur National Monument for their cooperation with permits to map within the boundaries of Dinosaur National Monument. In particular, the help and advice of Ann Elder, Steve Petersburg, and Dennis Huffman of the National Park Service are gratefully acknowledged. We also thank Scott Wilkins and Mike Wacker from Florida International University, Florida; Yehuda Eyal from Ben Gurion University, Israel; and Wayne Narr and Fred O'Toole from Chevron for their cooperative efforts during two field seasons at Split Mountain, Utah and Rangely, Colorado. Support for this work came from The Pennsylvania State University's Seal Evaluation Consortium (SEC), The Pennsylvania State University's Department of Geosciences Krynine Fund, The American Association of Petroleum Geologists Grant-in-Aid, and The United States–Israel Binational Science Foundation Grant No. 94-00396. We thank Steve Alhgren, Jim Evans, Don Fisher, John Lorenz, Kelly Rust, and Barry Voight for reviewing early versions of this paper.

References

Allmendinger, R.W., 1992. Fold and thrust tectonics of the western United States exclusive of the accreted terranes. In: Burchfiel, B.C., Lipman, P.W., Zoback, M.L. (Eds.), The Cordilleran Orogen: Conterminous U.S. Geological Society of America, Boulder, CO. The Geology of North America G-3, pp. 583–606.

Antonellini, M., Aydin, A., 1995. Effect of faulting on fluid flow in porous sandstones: geometry and spatial distribution. American Association of Petroleum Geologists Bulletin 79, 642–671.

Armstrong, R.L., 1968. Sevier orogenic belt in Nevada and Utah. Geological Society of America Bulletin 79, 429–458.

Aydin, A., 1978. Small faults formed as deformation bands in sandstone. Pure and Applied Geophysics 116, 913–930.

Bai, T., Pollard, D.D., 2000. Fracture spacing in layered rocks: a new explanation based on the stress transition. Journal of Structural Geology 22, 43–57.

Bobillo-Ares, N.C., Bastida, F., Aller, J., 2000. On tangential longitudinal strain folding. Tectonophysics 319, 53–68.

Brace, W.F., Bombolakis, E.G., 1963. A note on brittle crack growth in compression. Journal of Geophysical Research 68, 3709–3713.

Bradley, M.D., 1995. Timing of the Laramide rise of the Uinta Mountains, Utah and Colorado. In: Jones, R.W. (Ed.), Resources of Southwestern Wyoming. Wyoming Geological Association 1995 Field Conference Guidebook, pp. 31–44.

Byerlee, J., 1978. Friction in rocks. Pure and Applied Geophysics 116, 615–626.

Campbell, J.A., 1975. Structural geology and petroleum potential of the south flank of the Uinta Mountain uplift, northeastern Utah. Utah Geology 2, 129–132.

Corbett, K.P., Friedman, M., Spang, J., 1987. Fracture development and mechanical stratigraphy of Austin Chalk, Texas. American Association of Petroleum Geologists Bulletin 71, 17–28.

Cosgrove, J.W., Ameen, M.S., 2000. A comparison of the geometry, spatial organization and fracture patterns associated with forced folds and buckle folds: in Cosgrove, J.W., Ameen, M.S. (Eds.), Forced Folds and Fractures, Geological Society, London, Special Publications, 169, p. 7–21.

Cruikshank, K.M., Zhao, G., Johnson, A.M., 1991. Analysis of minor fractures associated with joints and faulted joints. Journal of Structural Geology 13, 865–886.

Davis, G.H., Bump, A.P., Barcia, P.E., Ahlgren, S.G., 1999. Conjugate Riedel deformation band shear zones. Journal of Structural Geology 22, 169–190.

Doelling, H.H., Graham, R.L., 1972. Eastern and northern Utah coal fields: Vernal, Henry mountains, Sego, La Sal-San Juan, Tabby Mountain, Coalville, Henry Fork, Goose Creek, and Lost Creek. Utah Geological and Mineral Survey, Monograph 2.

Dula Jr, W.F., 1981. Correlation between deformation lamellae, microfractures, and in situ stress measurements, White River uplift, Colorado. Geological Society of America Bulletin 92, 37–46.

Engelder, T., 1993. Stress Regimes in the Lithosphere. Princeton Press, Princeton.

Engelder, T., Geiser, P.A., 1980. On the use of regional joint sets as trajectories of paleostress fields during the development of the Appalachian Plateau, New York. Journal of Geophysical Research 85, 6319–6341.

Engelder, T., Gross, M.R., Pinkerton, P., 1997. An analysis of joint development in thick sandstone beds of the Elk Basin Anticline, Montana-Wyoming. In: Hoak, T.E., Klawitter, A.L., Blomquist, P.K. (Eds.), Fractured Reservoirs: Characterization and Modeling. Rocky Mountain Association of Geologists Guidebook, pp. 1–18.

Fischer, M.P., Wilkerson, M.S., 2000. Predicting the orientation of joints from fold shape: results of pseudo-three dimensional modeling and curvature analysis. Geology 28, 15–18.

Fischer, M.P., Gross, M.R., Engelder, T., Greenfield, R.J., 1995. Finite element analysis of the stress distribution around a pressurized crack in a layered elastic medium: implications for the spacing of fluid-driven joints in bedded sedimentary rock. Tectonophysics 247, 49–64.

Fisher, D.M., Anastasio, D.J., 1994. Kinematic analysis of a large-scale leading edge fold, Lost River Range, Idaho. Journal of Structural Geology 16, 337–354.

Fisher, R.S., 1953. Dispersion on a sphere. Proceedings of the Royal Society of London, A 217, 295–305.

Garfield, T.R., Hurley, N.F., Budd, D.A., 1992. Little Sand Draw field, Big Horn Basin, Wyoming: A hybrid dual-porosity and single-porosity reservoir in the Phosphoria Formation. American Association of Petroleum Geologists Bulletin 76, 371–391.

Ghosh, S.K., 1993. Structural Geology: Fundamentals and Modern Developments. Pergamon Press, Oxford.

Gregson, J.D., Erslev, E.A., 1997. Heterogeneous Laramide deformation in the Uinta Mountains, Colorado and Utah. In: Hoak, T.E., Klawitter, A.L., Blomquist, P.K. (Eds.), Fractured Reservoirs: Characterization and Modeling. Rocky Mountain Association of Geologists Guidebook, pp. 137–154.

Gries, R., 1983. North–south compression of Rocky Mountain foreland structures. In: Lowell, J.D. (Ed.), Rocky Mountain Foreland Basins and Uplifts: Denver Dolorado. Rocky Mountain Association of Geologists, pp. 9–32.

Gross, M.R., 1993. The origin and spacing of cross joints: examples from the Monterey Formation, Santa Barbara coastline, California. Journal of Structural Geology 15, 737–751.

Gross, M.R., 1995. Fracture partitioning: failure mode as a function of lithology in the Monterey Formation of coastal California. Geological Society of America Bulletin 107, 779–792.

Gross, M.R., Fischer, M.P., Engelder, T., Greenfield, R.J., 1995. Factors controlling joint spacing in interbedded sedimentary rocks: Integrating numerical models with field observations from the Monterey Formation, USA. In: Ameen, M.S. (Ed.), Fractography: Fracture Topography as a Tool in Fracture Mechanics and Stress Analysis. Geological Society Special Publication 92, pp. 215–233.

Gross, M.R., Bahat, D., Becker, A., 1997a. Relations between jointing and faulting based on fracture-spacing ratios and fault-slip profiles: a new method to estimate strain in layered rocks. Geology 25, 887–890.

Gross, M.R., Becker, A., Gutierrez-Alonso, G., 1997b. Transfer of displacement from multiple slip zones to a single detachment due to rigid block rotation: Example from the Dead Sea Rift, Israel. Geological Society of America Bulletin 109, 1021–1035.

Grout, M.A., Verbeek, E.R., 1992. Fracture history of the Divide Creek and Wolf Creek Anticlines and its relation to Laramide basin-margin tectonism, Southern Piceance Basin, Northwestern Colorado. U.S. Geological Survey Bulletin 1787-Z.

Grout, M.A., Verbeek, E.R., 1992. Joint-history summary and orientation data for Upper Cretaceous sandstones. Rawlins and Rock Springs Uplifts, Washakie Basin, southern Wyoming. U.S. Geological Survey Open-File Report 92-388.

Hancock, P.L., 1985. Brittle microtectonics: principles and practice. Journal of Structural Geology 7, 437–457.

Hancock, P.L., Engelder, T., 1989. Neotectonic joints. Geological Society of America Bulletin 101, 1197–1208.

Hansen, W.R., 1984. Post-Laramide tectonic history of the eastern Uinta Mountains, Utah, Colorado, and Wyoming. The Mountain Geologist 21, 5–29.

Hansen, W.R., 1986. History of faulting in the eastern Uinta Mountains, Colorado and Utah. In: Stone, D.S. (Ed.), New interpretations of northwest Colorado geology. Rocky Mountain Association of Geologists — 1986 Symposium, pp. 229–246.

Harper, M.L., 1964. Mechanics of basement deformation in Glenwood Canyon, Colorado. Mountain Geologist 3, 185–192.

Harris, J.F., Taylor, G.L., Walper, J.L., 1960. Relation of deformational structures in sedimentary rocks to regional and local structure. American Association Petroleum Geologists Bulletin 44, 1853–1873.

Hennings, P.H., Olson, J.E., Thompson, L.B., 2000. Combining outcrop data and three-dimensional structural models to characterize fractured reservoirs: an example from Wyoming. American Association of Petroleum Geologists Bulletin 84, 830–849.

Hintze, L.F., 1988. Geologic History of Utah. Brigham Young University Studies Special Publication 7.

Hucka, B., 1991. Analysis and regional implication of cleat and joint systems in selected coal seams. Carbon, Emery, Sanpete, Sevier, and Summit counties, Utah: Special Studies — Utah Geological and Mineral Survey Report 74.

Ingraffea, A.R., 1987. Theory of crack initiation and propagation in rock. In: Atkinson, B. (Ed.), Fracture Mechanics of Rock. Academic Press, London, pp. 71–110.

Jaeger, J.C., Cook, N.G.W., 1976. Fundamentals of Rock Mechanics. 2nd ed. Chapman and Hall, London.

Jamison, W.R., 1987. Geometric analysis of fold development in overthrust terranes. Journal of Structural Geology 9, 207–219.

Jamison, W.R., Stearns, D.W., 1982. Tectonic deformation of Wingate sandstone, Colorado National Monument. American Association Petroleum Geologists 66, 2584–2608.

Ji, S., Saruwatari, K., 1998. A revised model for the relationship between joint spacing and layer thickness. Journal of Structural Geology 20, 1495–1508.

La Pointe, P.R., Hudson, J.A., 1985. Characterization and interpretation of rock mass joint patterns. Geological Society of America Special Paper, 199.

Ladeira, F.L., Price, N.J., 1981. Relationship between fracture spacing and bed thickness. Journal of Structural Geology 3, 179–183.

Laubach, S.E., 1992. Fracture networks on selected Cretaceous sandstones of the Green River and San Juan Basins, Wyoming, New Mexico, and Colorado. In: Schmoker, J.W., Coalson, E.B., Brown, C.A. (Eds.), Geologic Studies Relevant to Horizontal Drilling: Examples from Western North America. Rocky Mountain Association of Geologists Guidebook, pp. 115–127.

Laubach, S.E., Lorenz, J.C., 1992. Preliminary assessment of natural fracture patterns in Frontier Formation sandstones, Southwest Wyoming. In: Mullen, C.E. (Ed.), Rediscover the Rockies. Wyoming Geological Association Forty-Third Field Conference Guidebook, pp. 87–96.

Laubach, S.E., Clift, S.J., Hill, R.E., Fix, J., 1992a. Stress directions in Cretaceous Frontier Formation, Green River Basin, Wyoming. In: Mullen, C.E. (Ed.), Rediscover the Rockies. Wyoming Geological Association Forty-Third Field Conference Guidebook, pp. 75–86.

Laubach, S.E., Tyler, R., Ambrose, W.A., Tremain, C.M., Grout, M.A., 1992b. Preliminary map of fracture patterns in coal in the Western United States. In: Mullen, C.E. (Ed.), Rediscover the Rockies. Wyoming Geological Association Forty-Third Field Conference Guidebook, pp. 253–267.

Lawn, B., 1993. Fracture of Brittle Solids. 2nd ed. Cambridge University Press, Cambridge.

Lemiszki, P.T., Landers, J.D., Hatcher, R.D., 1994. Controls on hinge-parallel extension fracturing in single-layer tangential–longitudinal strain folds. Journal of Geophysical Research 99, 22,027–22,041.

Lisle, R.J., 1994. Detection of zones of abnormal strains in structures using gaussian curvature analysis. American Association of Petroleum Geologists Bulletin 78, 1811–1819.

Lorenz, J.C., 1995. Stresses and fractures in the Frontier Formation, Green River Basin, predicted from basin-margin tectonic element interactions. In: Jones, R.W. (Ed.), Resources of Southwestern Wyoming. Wyoming Geological Association 1995 Field Conference Guidebook, pp. 45–60.

Lorenz, J.C., Finley, S., 1991. Regional fractures I: A mechanism for the formation of regional fractures at depth in flat-lying reservoirs. American Association Petroleum Geologists Bulletin 75, 1714–1737.

Lorenz, J.C., Hill, R., 1994. Subsurface Fracture Spacing: Comparison of Inferences from Slant/Horizontal and Vertical Cores. Society of Petroleum Engineers (SPE) Formation Evaluation, pp. 66–72.

Lorenz, J.C., Teufel, L.W., Warpinski, N.R., 1991. Regional fractures: II. A mechanism for the formation of regional fractures at depth in flat-lying reservoirs. American Association Petroleum Geologists Bulletin 75, 1714–1737.

Maschmeyer, E.P., Cooke, M.L., 2000. Do primary joint patterns at the northern termination of Sheep Mountain anticline, WY, reflect current or former structural position. Geological Society of America Abstracts with Program 32, A-228.

McCaleb, J.A., Wayhan, D.A., 1969. Geologic reservoir analysis, Mississippian Madison Formation, Elk Basin Field, Wyoming-Montana. American Association of Petroleum Geologists Bulletin 53, 2094–2113.

McElhinny, M.W., 1964. Statistical significance of the fold test in paleomagnetism. Geophysical Journal of Astronomical Society 8, 338–340.

Melton, F.A., 1929. A reconnaissance of the joint systems in the Ouachita Mountains and central plains of Oklahoma. Journal of Geology 37, 729–746.

Morel, J.A., Bursk, P.H., Dlouhy, D.L., 1986. An interpretation of the subsurface structural style of the Beaver Creek anticline, Moffat and Routt Counties, Colorado. In: Stone, D.E. (Ed.), New Interpretations of Northwest Colorado Geology. Rocky Mountain Association of Geologists Guidebook, pp. 195–202.

Murray, F.N., 1967. Jointing in sedimentary rocks along the Grand Hogback Monocline. Journal of Geology 75, 340–350.

Murray, G.H., 1968. Quantitative Fracture Study — Sanish Pool, McKenzie Co., North Dakota. American Association of Petroleum Geologists Bulletin 52, 57–65.

Narr, W., 1991. Fracture density in the deep subsurface: Techniques with application to Point Arguello Oil Field. American Association of Petroleum Geologists Bulletin 75, 1300–1323.

Narr, W., 1998. Quantifying subsurface fracture sets: collecting and analyzing data with simulation in mind. In: Hoak, T.E. (Ed.), Fractured Reservoirs: Practical Exploration and Development Strategies. Rocky Mountain Association of Geologists, pp. 137–155.

Narr, W., Suppe, J., 1991. Joint spacing in sedimentary rocks. Journal of Structural Geology 13, 1037–1048.

Nickelsen, R.P., Hough, V.D., 1967. Jointing in the Appalachian Plateau of Pennsylvania. Geological Society of America Bulletin 78, 609–630.

Novoa, E., Mount, V., Suppe, J., 1998. Map-view interference of monoclinal folds: Journal of Structural Geology, v. 4, p. 339–353.

Peterson, F., 1986. Jurassic paleotectonics in the west-central part of the Colorado Plateau, Utah, and Arizona. In: Peterson, J.A. (Ed.), Paleotectonics and Sedimentation in the Rocky Mountain Region, United States. American Association of Petroleum Geologists Memoir 41, pp. 563–593.

Peterson, F., Turner-Peterson, C.E., 1987. The Morrison Formation of the Colorado Plateau, recent advances in sedimentology, stratigraphy, and paleotectonics. Hunteria 2, 18.

van der Pluijm, B.A., Marshak, S., 1997. Earth Structure: An Introduction to Structural Geology and Tectonics. McGraw Hill, New York.

Pollard, D.D., Segall, P., 1987. Theoretical displacements and stresses near fractures in rock: with applications to faults, joints, veins, dikes, and solution surfaces. In: Atkinson, B. (Ed.), Fracture Mechanics of Rock. Academic Press, Orlando, pp. 227–350.

Pollard, D.D., Aydin, A., 1988. Progress in understanding jointing over the past century. Geologic Society of America Bulletin 100, 1181–1204.

Powell, C.McA., 1974. Timing of slaty cleavage during folding of Precambrian rocks, northwest Tasmania. Bulletin of the Geological Society of America 85, 1043–1060.

Price, N.J., Cosgrove, J.W., 1990. Analysis of Geological Structures. Cambridge University Press, Cambridge.

Priest, S.D., Hudson, J.A., 1976. Discontinuity spacing in rock. International Journal of Rock Mechanics Mining Science and Geomechanics Abstracts 13, 135–148.

Ramsay, J.G., 1967. Folding and Fracturing of Rocks. McGraw-Hill, New York.

Ramsay, J.G., Huber, M.I., 1987. The Techniques of Modern Structural Geology: Volume 2: Folds and Fractures. Academic Press, Orlando.

Richard, J.J., 1986. Interpretation of a seismic section across the Danforth Hills anticline (Maudlin Gulch) and Axial Arch in northwestern Colorado. In: Stone, D.E. (Ed.), New Interpretations of Northwest Colorado Geology. Rocky Mountain Association of Geologists Guidebook, pp. 191–196.

Ritzma, H.R., 1969. Tectonic resume, Uinta Mountains. In: Lindsay, J.B. (Ed.), Geologic Guidebook of the Uinta Mountains: Utah's Maverick Range. Intermountain Association of Geologists 16th Annual Field Conference Guidebook, pp. 57–63.

Rowley, P.D., Hansen, W.R., 1979. Geologic map of the Split Mountain Quadrangle. Uintah County, Utah. U.S. Geological Survey Geological Quadrangle Map GQ-1515, scale 1:24,000.

Rowley, P.D., Kinney, D.M., Hansen, W.R., 1979. Geologic map of the Dinosaur Quarry Quadrangle. Uinta County, Utah. U.S. Geological Survey Geological Quadrangle Map GQ-1513, scale 1:24,000.

Silliphant, L.J., 1998. Regional and fold-parallel joint distribution at Split Mountain anticline, Utah: a study of the relationship between joint development and 2-D curvature in Laramide folds. MS Thesis. Pennsylvania State University.

Srivastava, D., Engelder, T., 1990. Crack-propagation sequence and pore-fluid conditions during fault-bend folding in the Appalachian Valley and Ridge. Geological Society of America 102, 116–128.

Stearns, D.S., 1978. Faulting and forced folding in Rocky Mountains foreland. In: Matthews III, V. (Ed.). Laramide Folding Associated with Basement Block Faulting in the Western United States. Geological Society of America Memoir 151, pp. 1–37.

Stone, D.S., 1986. Seismic and borehole evidence for important pre-Laramide faulting along the Axial Arch in northwest Colorado geology. In: Stone, D.E. (Ed.), New Iinterpretations of Northwest Colorado Geology. Rocky Mountain Association of Geologists Guidebook, pp. 19–36.

Stone, D.S., 1993. Basement-involved thrust -generated folds as seismically imaged in the subsurface of the central Rocky Mountain foreland. In: Schmidt, C.J., Chase, R.B., Erslev, E.A. (Eds.), Laramide Basement Deformation in the Rocky Mountain Foreland of the Western United States. Geological Society of America Special Paper 280, pp. 271–318.

Suppe, J., 1985. Principles of Structural Geology. Prentice-Hall, Englewood Cliffs.

Treagus, J.E., Treagus, S.W., 1981. Folds and strain ellipsoid. Journal of Structural Geology 3, 1–17.

Tremain, C.M., Tyler, R., 1997. Cleat, fracture, and stress patterns in the Piceance Basin, Colorado: controls on coalbed methane producibility. In: Hoak, T.E., Klawitter, A.L., Blomquist, P.K. (Eds.), Fractured Reservoirs: Characterization and Modeling. Rocky Mountain Association of Geologists Guidebook, pp. 103–114.

Tyler, R., Tremain, C.M., 1993. Tectonic evolution, stratigraphic setting, and coal fracture patterns of the Sand Wash Basin. In: Kaiser, W.R., Scott, A.R., Hamilton, D.S., Tyler, R., McMurray, R.G., Zhou, N., Tremain, C.M. (Eds.), Geologic and Hydrologic Controls on Coalbed Methane: Sand Wash Basin. Bureau of Economic Geology, The University of Texas at Austin, pp. 3–19. Topical report prepared for the Gas research Institute under contract no. 5091-214-2261 (GRI-92/0420).

Tyler, R., Ambrose, W.A., Scott, A.R., Kaiser, W.R., 1992a. Evaluation of the coalbed methane potential in the Greater Green River, Piceance, Powder River, and Raton Basins. In: Mullen, C.E. (Ed.), Rediscover the Rockies. Wyoming Geological Association Forty-Third Field Conference Guidebook, pp. 296–302.

Tyler, R., Kaiser, W.R., Ambrose, W.A., Scott, A.R., Laubach, S.E., Ayers Jr, W.B., 1992b. Coalbed methane characteristics in the foreland of the Cordilleran thrust belt, western United States. In: Beamish, B.B., Gamson, P.D. (Eds.), Symposium on Coalbed Methane Research and Development in Australia. James Cook University of North Queensband (Coalseam Gas Research Institute), pp. 11–32.

Untermann, G.E., Untermann, B.R., 1949. Geology of Green and Yampa River canyons and vicinity, Dinosaur National Monument, Utah and Colorado. American Association Petroleum Geologists Bulletin 33, 683–694.

Untermann, G.E., Untermann, B.R. 1955. Geology of the eastern end of the Uinta Mountains, Utah-Colorado. Guidebook to the Geology of Northwest Colorado, Sixth Annual Field Conference, pp. 18–20.

Verbeek, E.R., Grout, M.A., 1992. Structural Evolution of Gilsonite Dikes, Eastern Uinta Basin, Utah. In: Fouch, T.D., Nuccio, V.F., Chidsey Jr, T.C. (Eds.), Hydrocarbon and Mineral Resources of the Uinta Basin, Utah and Colorado. Utah Geological Association Guidebook 20, pp. 237–255.

Verbeek, E.R., Grout, M.A., 1997. Joint networks in reservoir rocks: case studies of prediction at depth. In: Hoak, T.E., Klawitter, A.L., Blomquist, P.K. (Eds.), Fractured Reservoirs: Characterization and Modeling. Rocky Mountain Association of Geologists Guidebook, pp. 115–129.

Wilkins, S.J., Gross, M.R., Wacker, M., Eyal, Y., Engelder, T., 2001. Faulted Joints: kinematics, scaling relations, and criteria for their identification. Journal of Structural Geology 23, 315–327.

Withjack, M.O., Olson, J., Peterson, E., 1990. Experimental models of extensional forced folds. American Association Petroleum Geologists Bulletin 74, 1038–1054.

Wiltschko, D.V., Dorr Jr, J.A., 1983. Timing of deformation in overthrust belt and foreland of Idaho, Wyoming, and Utah. American Association Petroleum Geologists Bulletin 67, 1304–1322.